$t\bar{t} + b\bar{b}$ Measurements from ATLAS and CMS

Egor Antipov

Stony Brook University, New York

on behalf of the ATLAS and CMS collaborations

17th International Workshop on Top Quark Physics (TOP2024)

September 22nd - 27th, Saint-Malo, Brittany, France.

Talk Outline

- Motivation for $\mathrm{t\bar{t}} + \mathrm{b\bar{b}}$ measurements at ATLAS and CMS.

- Measurement of $\mathrm{t\bar{t}}$ production in association with additional *b*-jets in the $e\mu$ final state in proton-proton collisions at $\sqrt{s} = 13$ TeV with the ATLAS detector (arXiv:2407.13473, submitted to JHEP):
  - Analysis strategy.
  - $\mathrm{t\bar{t}}$+light and $\mathrm{t\bar{t}}$+c background estimate: flavor fit.
  - *b*-jets assignment to tops algorithm.
  - Fiducial and differential cross-section measurements results.

- Inclusive and differential cross section measurements of $\mathrm{t\bar{t}b\bar{b}}$ production in the lepton+jets channel at $\sqrt{s} = 13$ TeV [with the CMS detector] (JHEP 05 (2024) 042):
  - Analysis strategy.
  - Ancillary variable for the fit.
  - *b*-jets assignment as the additional pair.
  - Fiducial and differential cross-section measurements results.

- Summary.

$t\bar{t}b\bar{b}$ Cross-section Measurement Motivation

Better understanding of the QCD modeling of heavy flavor jets produced with top quark pair:

- Non-trivial predictions due to very different scales involved starting from m_{top} down to momenta of soft additional radiations.
    - Modeling of additional *b*-jets available at various state-of-the-art NLO ME+PS predictions.

Important background for many processes: $t\bar{t}H(b\bar{b})$, four tops and others.

arXiv:2407.13473

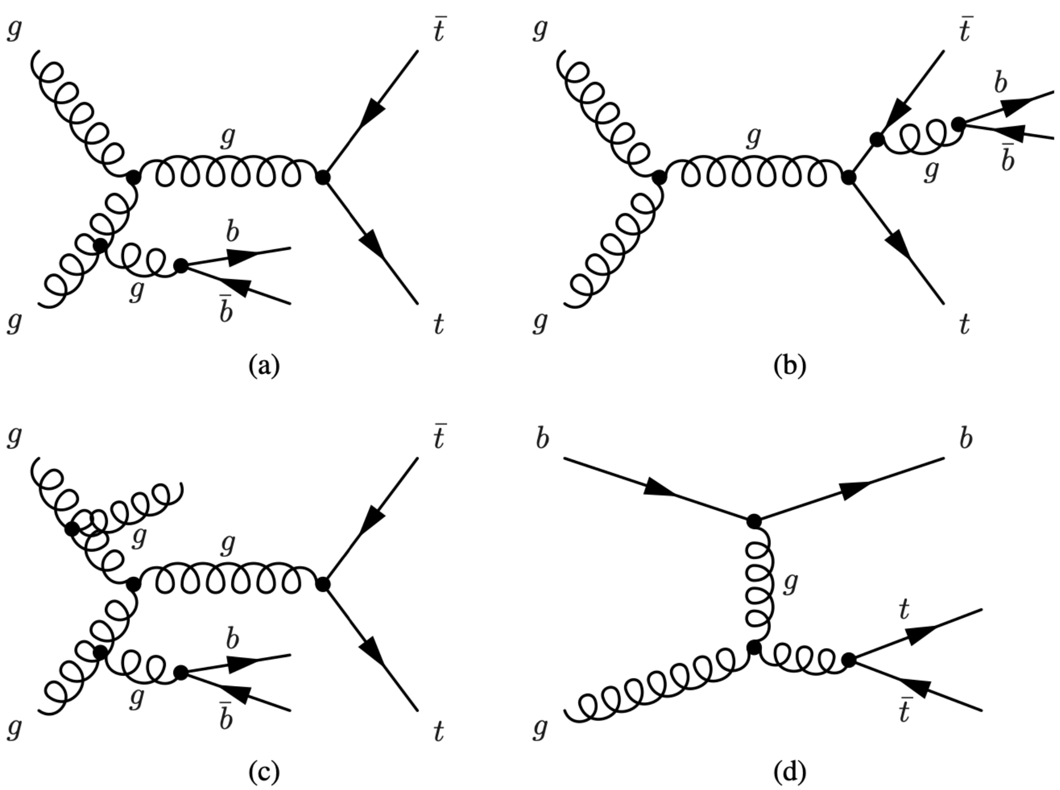

Examples of Feynman diagrams of QCD processes leading to $t\bar{t}b\bar{b}$ final state:

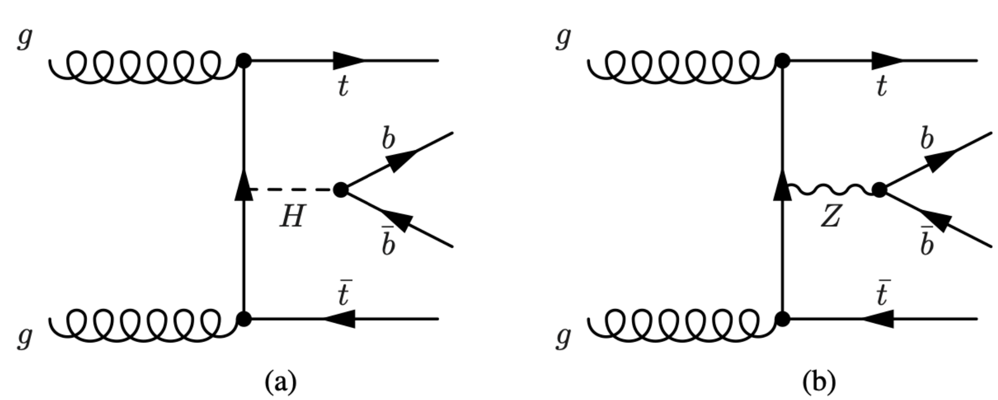

arXiv:2407.13473

Examples of Feynman diagrams of electroweak processes leading to $t\bar{t}b\bar{b}$ final state:

Measurement of $t\bar{t}$ production in association with additional b-jets in the $e\mu$ final state in proton-proton collisions at $\sqrt{s} = 13$ TeV with the ATLAS detector

arXiv:2407.13473

Analysis Strategy

Particle-level measurement in the $e\mu$ (OS) channel:

- Integrated fiducial cross-section in multiple regions: $e\mu$ + ≥3*b* | ≥4*b* | ≥3*b* + ≥1 *l/c* | ≥4*b*+≥1 *l/c*.
- Normalized differential cross-sections as a function of various variables in the 4 phase spaces.
  - Some observables are defined after assigning *b*-jets to the top quarks or the additional jets using kinematic information (full list of observables is in backup).

The data are unfolded to the particle level after subtracting the estimated background and correcting for the detector effects. IBU, 4 iterations. Compared to various MC predictions.

Background corrections using semi-data-driven method:

- Fake leptons (small background, in backup).
- Miss-tagged $t\bar{t}$+light jets and $t\bar{t}$+c jets estimation.

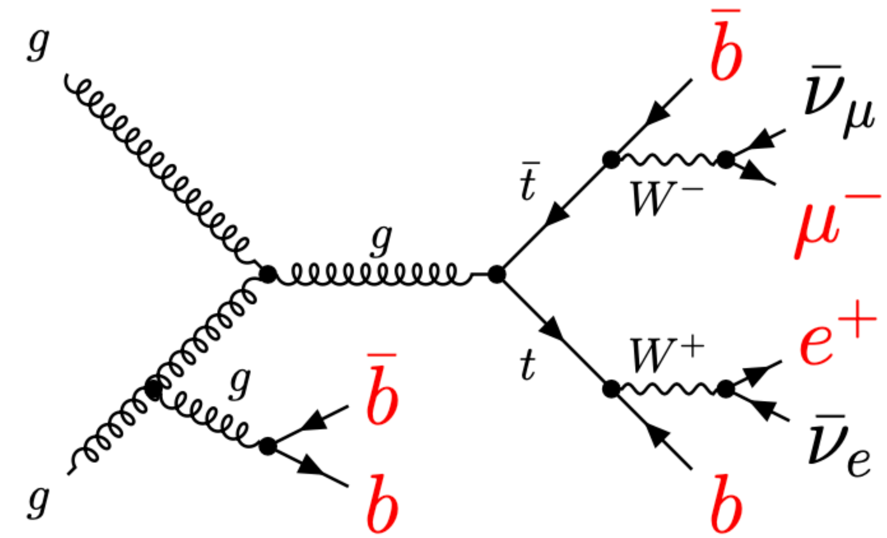

arXiv:2407.13473

Event yields for the events before any flavor composition scale factors are applied to $t\bar{t}$ events are presented.

Process	$\geq 2j, 2b$@77%	$\geq 3j, 3b$@77%	$\geq 4j, \geq 4b$@77%
$t\bar{t}$ +*b*-jets	4100 ± 790	3550 ± 650	474 ± 99
$t\bar{t}c$	11600 ± 2200	2190 ± 430	57 ± 15
$t\bar{t}l$	263000 ± 33000	2080 ± 440	25 ± 15
Wt	9100 ± 1800	227 ± 94	14 ± 11
$t\bar{t}V$	740 ± 230	94 ± 30	16.3 ± 5.1
$t\bar{t}H$	180 ± 22	108 ± 13	37.2 ± 5.3
Non-prompt lepton	340 ± 210	37 ± 20	10.9 ± 6.1
Z/γ^*+jets	96 ± 38	3.4 ± 1.4	0.15 ± 0.09
Diboson	85 ± 43	3.0 ± 1.5	0.11 ± 0.07
Others	41 ± 20	16.4 ± 8.2	6.4 ± 2.9
Total predicted	290000 ± 35000	8300 ± 1300	640 ± 120
Observed	281213	10235	798

Objects and Event Selection

Detector level events selection:

arXiv:2407.13473

- Single lepton triggers:
  - $p_T > 24\ (26)$ GeV for 2015 (2016-2018).
- Exactly one electron and one muon
  - Opposite signs, isolated leptons.
  - $p_T > 28$ GeV, $|\eta| < 2.5$.
  - $m_{e\mu} > 15$ GeV to reject low-mass τ.

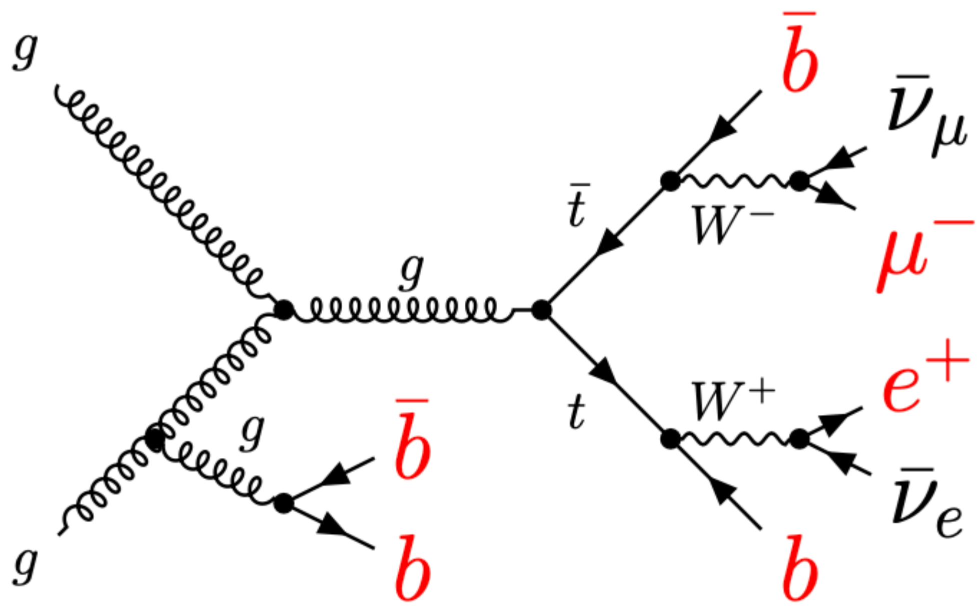

- At least 2 jets:
  - anti-k_t $(R = 0.4)$ on particle flow constituents.
  - $p_T > 25$ GeV, $|\eta| < 2.5$.
- At least 2 *b*-tagged jets:
  - DL1r *b*-tagging algorithm (deep NN), baseline working point with 77% efficiency.
- **Similar particle-level section criteria to define fiducial phase space.**

$t\bar{t}$+jets Flavors Fit: Setup

Mistagged jets in $t\bar{t}$+light-jets and $t\bar{t}$+c-jets events (categorized depending on the number of particle *b*/c/light-jets) contribute as significant background to $t\bar{t}$+*b*-jets measurement.

- 3j3b: $\sim 50\,\%$ of events selected at the detector level have at least 3 *b*-jets at the particle level.
- Perform template fits to data to extract scale factors $\alpha_{b/c/l}$ using the 3^{rd} (and the 4^{th}) highest *b*-tagging discriminant score jet in events with ≥3 (4) *b*-jets.

arXiv:2407.13473

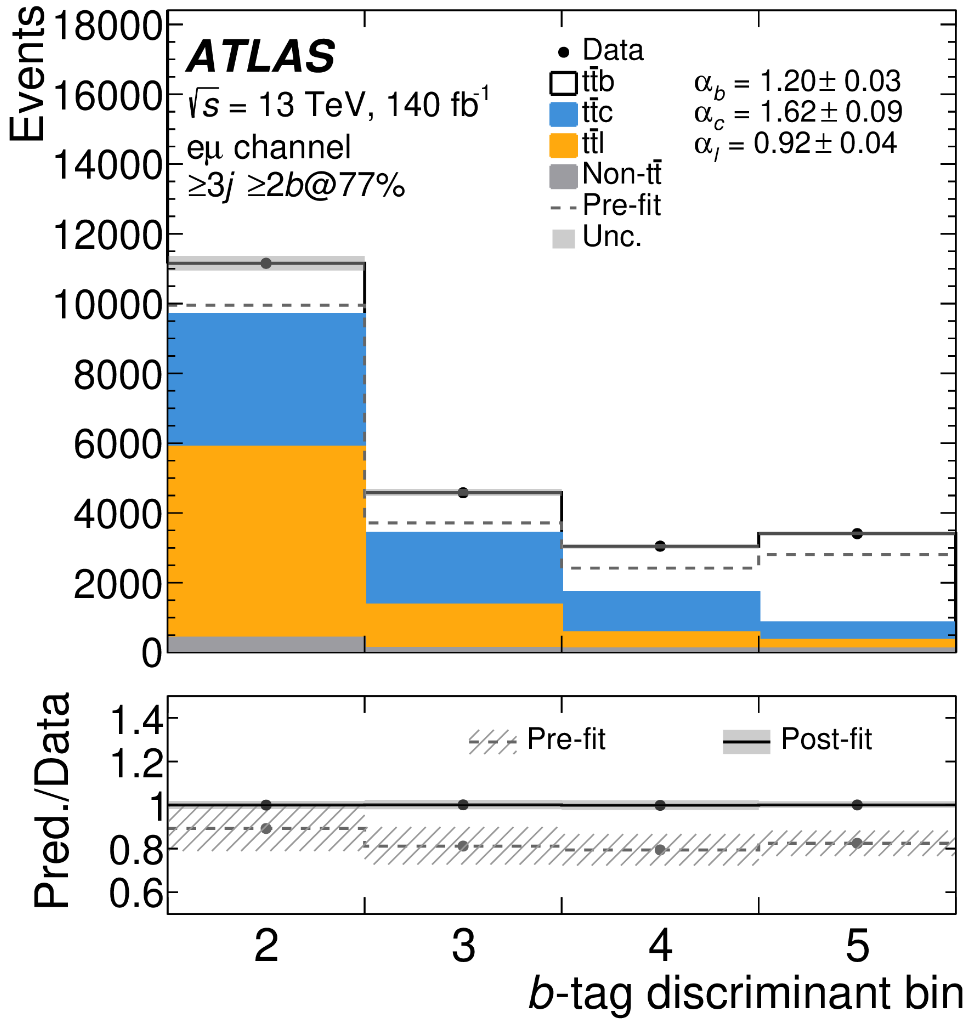

Two types of fits are performed:

1. ***Global*** (≥3 jets: ≥2*b* region, inclusive in jet p_{T} > 25 GeV): the nominal approach to correct the normalization of individual $t\bar{t}j$ components.
2. ***Kinematic-dependent*** (==3 and ≥4 jets regions: ≥2*b*, sliced in p_{T} of the 3^{rd} *b*-tag discriminant ranked jet): improves normalization and shape but can't be applied to the truth particle level events (due to potential bias). Used to evaluate the systematic uncertainty accounting for the shape effects of the $t\bar{t}c$ and $t\bar{t}l$ background.

The data are described much better by the prediction after the individual $t\bar{t}j$ components are corrected.

b-jets Origins Classification

Create all possible permutations of *b*-jets in an event.

- In events with ≥4 *b*-jets consider only the 4 highest p_{T} *b*-jets.

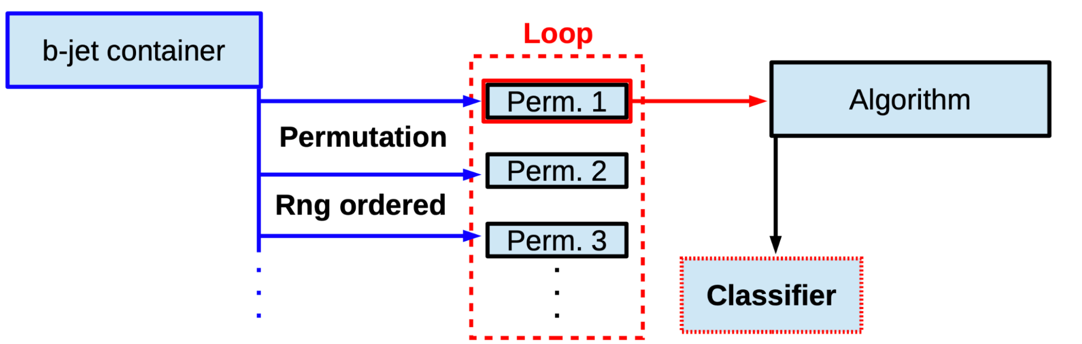

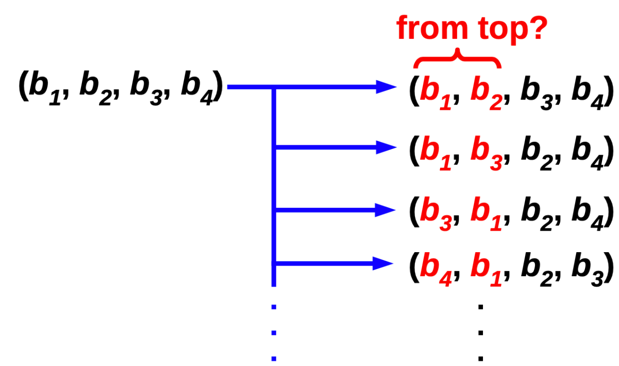

The permutation with the minimal $-\ln(w)$ is chosen, and the first two *b*-jets in the permutation are assigned to top quarks:

$$-\ln w = \begin{cases} \left(\Delta R_{\ell 1 b1} - \Delta R^{\min}_{\ell 1 b}\right)^2 + \left(\Delta R_{\ell 2 b2} - \Delta R^{\min}_{\ell 2 b}\right)^2 + \left(\max(\Delta R_{b1b3}, \Delta R_{b2b3}) - \Delta R^{\max}_{bb}\right)^2 & \text{if } N_{b\text{-jets}} = 3, \\ \left(\Delta R_{\ell 1 b1} - \Delta R^{\min}_{\ell 1 b}\right)^2 + \left(\Delta R_{\ell 2 b2} - \Delta R^{\min}_{\ell 2 b}\right)^2 + \left(\Delta R_{b3b4} - \Delta R^{\min}_{bb}\right)^2 & \text{if } N_{b\text{-jets}} \geq 4, \end{cases}$$

Fraction of events with correctly assigned *b*-jets:

- By the algorithm: $53\ \%\ (56\%)$ in $t\bar{t}$ events with at least 3 (4) *b*-jets.
- Selecting the leading p_{T} *b*-jets: $42\ \%\ (27\%)$.

The probabilities of correct assignment of *b*-jet(s) in a given bin of the measured observable ranges from $50\ \%$ to $85\ \%$ ($40\ \%$ to $75\ \%$).

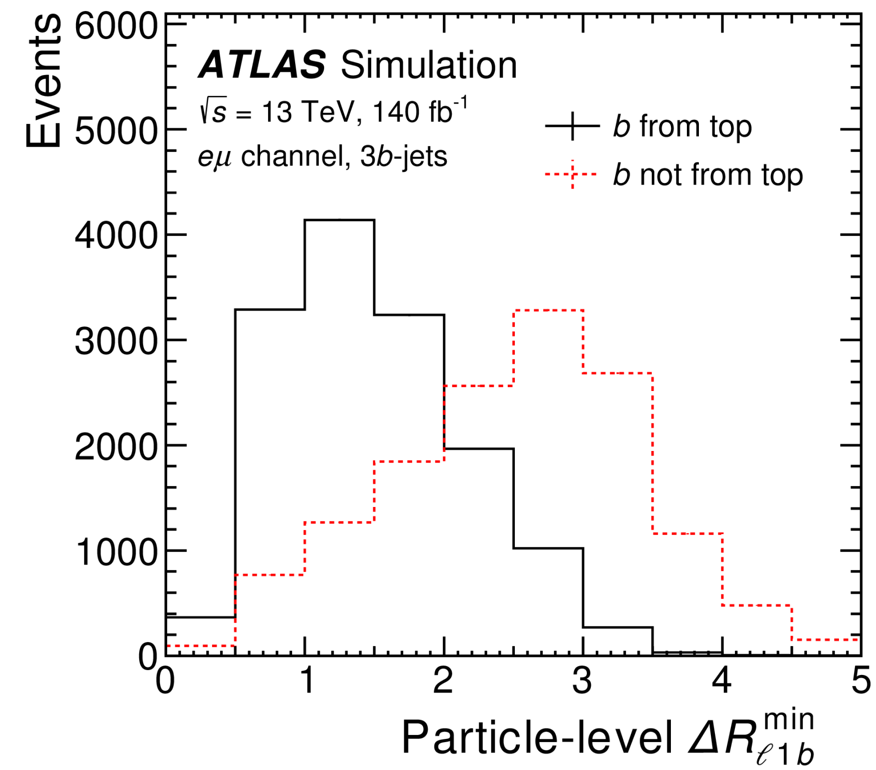

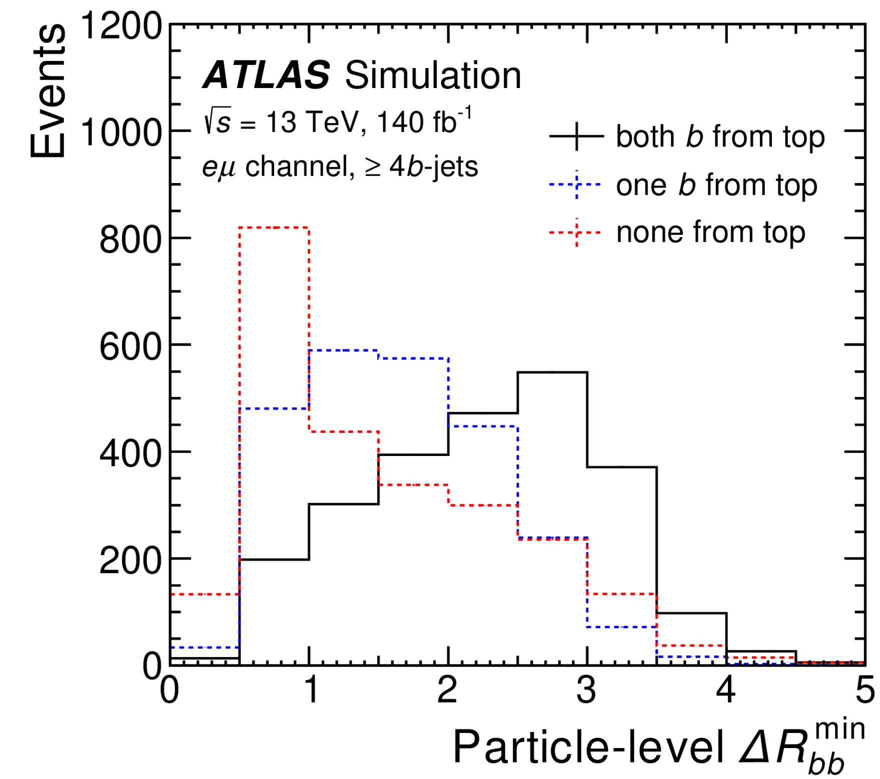

arXiv:2407.13473

Unfolding Formula

The unfolding procedure for an observable X at particle level is summarized by the following expression:

$$N^i_{\text{unfold}} = \frac{1}{f^i_{\text{eff}}} \sum_k \mathcal{M}^{-1}_{ik} f^k_{\text{accept}} f^k_{t\bar{t}b} (N^k_{\text{data}} - N^k_{\text{bkg}})$$

Correction factors:

reconstruction efficiency

$$f^i_{\text{eff},t\bar{t}b} = \frac{\mathcal{S}^i_{t\bar{t}b,\text{part}\wedge\text{reco}}}{\mathcal{S}^i_{t\bar{t}b,\text{part}}}$$

fiducial acceptance

$$f^k_{\text{accept},t\bar{t}b} = \frac{\mathcal{S}^k_{t\bar{t}b,\text{reco}\wedge\text{part}}}{\mathcal{S}^k_{t\bar{t}b,\text{reco}}}$$

ttj flavor composition

$$f^k_{t\bar{t}b} = \frac{\mathcal{S}^k_{t\bar{t}b,\text{reco}}}{\mathcal{S}^k_{t\bar{t}b,\text{reco}} + \mathcal{B}^k_{t\bar{t}b,\text{reco}}}$$

Results from the unfolded distributions are presented in terms of a relative differential cross section:

$$\frac{1}{\sigma^{\text{fid}}} \cdot \frac{\mathrm{d}\sigma^{\text{fid}}}{\mathrm{d}X^i} = \frac{N^i_{\text{unfold}}}{\Delta X^i \sum_i N^i_{\text{unfold}}}$$

arXiv:2407.13473

Fiducial Cross-Section Measurements: Results

$t\bar{t}$ (5FS) NLO ME+PS slightly under predicts additional *b*-jets production.

Sherpa with one parton at NLO (5FS) under predicts events with ≥3 and ≥4 *b*-jets.

Powheg $t\bar{t}b\bar{b}$ predictions in 4FS describe data well in the ≥4 *b*-jets region.

Sherpa $t\bar{t}b\bar{b}$ remains consistent with data in all four phase spaces.

Measured and predicted fiducial cross-section results

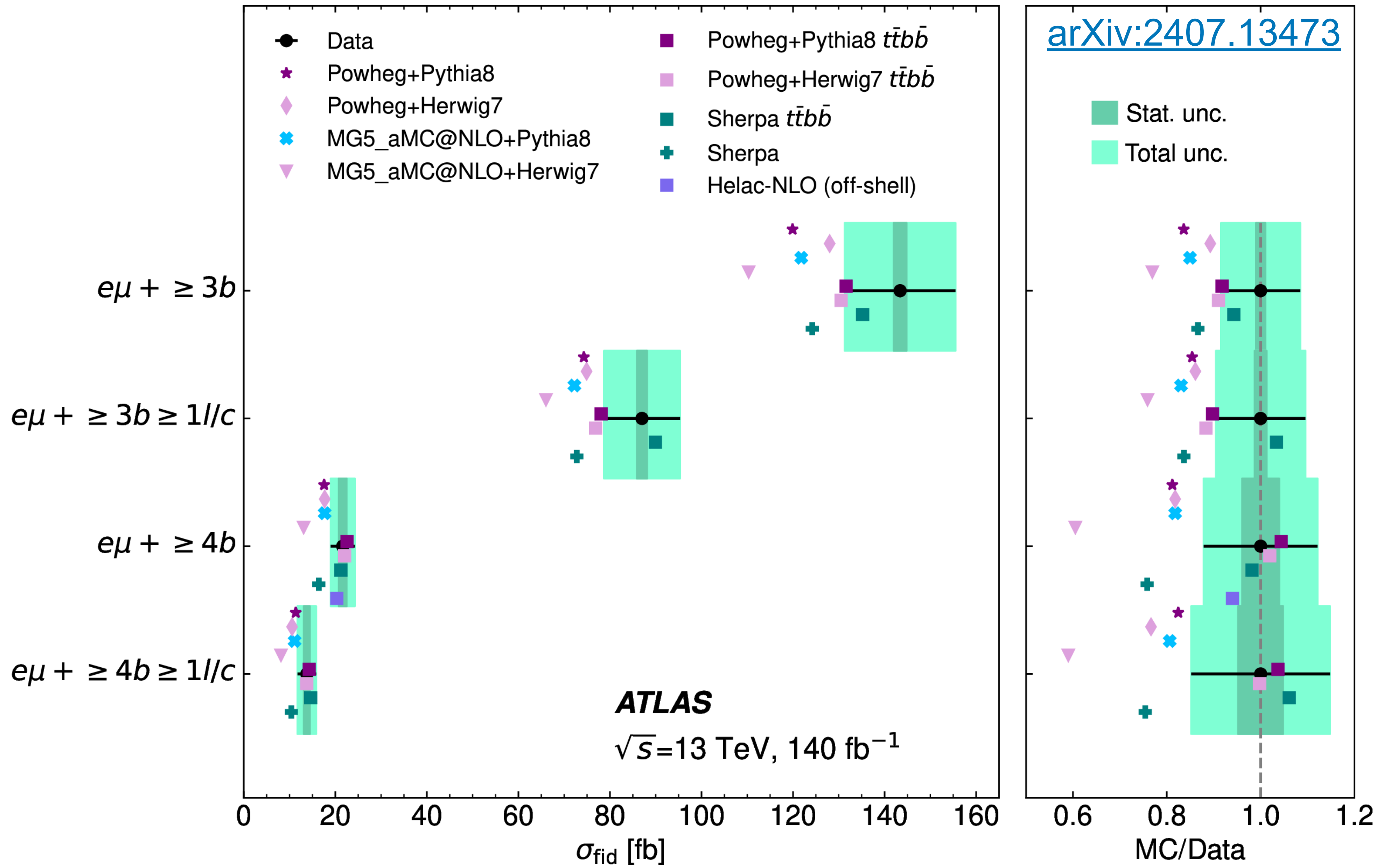

Overall, 4FS generators predictions agree with data better than 5FS.

Fiducial Cross-Section Measurements: Systs

Source	Fiducial cross-section phase space			
	$\geq 3b$ Unc. [%]	$\geq 3b \geq 1l/c$ Unc. [%]	$\geq 4b$ Unc. [%]	$\geq 4b \geq 1l/c$ Unc. [%]
Data statistical uncertainty	1.0	1.2	3.9	4.8
Luminosity	0.8	0.8	0.8	0.8
Jet	3.4	5.2	6.6	8.5
b-tagging	5.1	4.9	6.5	6.4
Lepton and trigger	1.4	1.4	1.2	1.2
Pile-up	0.9	0.7	0.6	0.3
$t\bar{t}c/t\bar{t}l$ fit variation	1.7	1.7	0.8	0.8
$t\bar{t}c/t\bar{t}l$ shape variation	0.2	0.5	0.3	1.6
$t\bar{t}H/t\bar{t}V$ and non-$t\bar{t}$ background	1.1	1.1	2.2	2.4
Detector+background total syst.	6.7	7.6	9.7	11.2
Parton shower and hadronisation	2.9	3.5	1.5	3.6
μ_R and μ_F scale variations	0.7	0.6	0.2	0.3
Matrix element matching (p_T^{hard})	1.3	1.1	4.8	7.0
h_{damp}	1.8	1.5	2.9	3.2
ISR	0.1	0.4	0.2	0.3
FSR	3.1	3.6	3.3	3.1
RecoilToTop	1.8	1.9	2.4	3.4
PDF	0.2	0.2	0.1	0.1
NNLO reweighting	0.6	0.5	0.5	0.5
MC statistical uncertainty	0.2	0.2	0.5	0.6
$t\bar{t}$ modelling total syst.	5.2	5.7	7.2	9.7
Total syst.	8.5	9.6	12.1	14.8
Total	8.5	9.6	12.7	15.5

arXiv:2407.13473

Differential Cross-Section Measurements

Right: Quantitative comparisons with predictions show good agreement for *most* observables within the uncertainties, and the differences among various predictions are small.

Left: Example of $p_{\mathrm{T}}(b_1^{\mathrm{add}})$ in events with ≥3 *b*-jets.

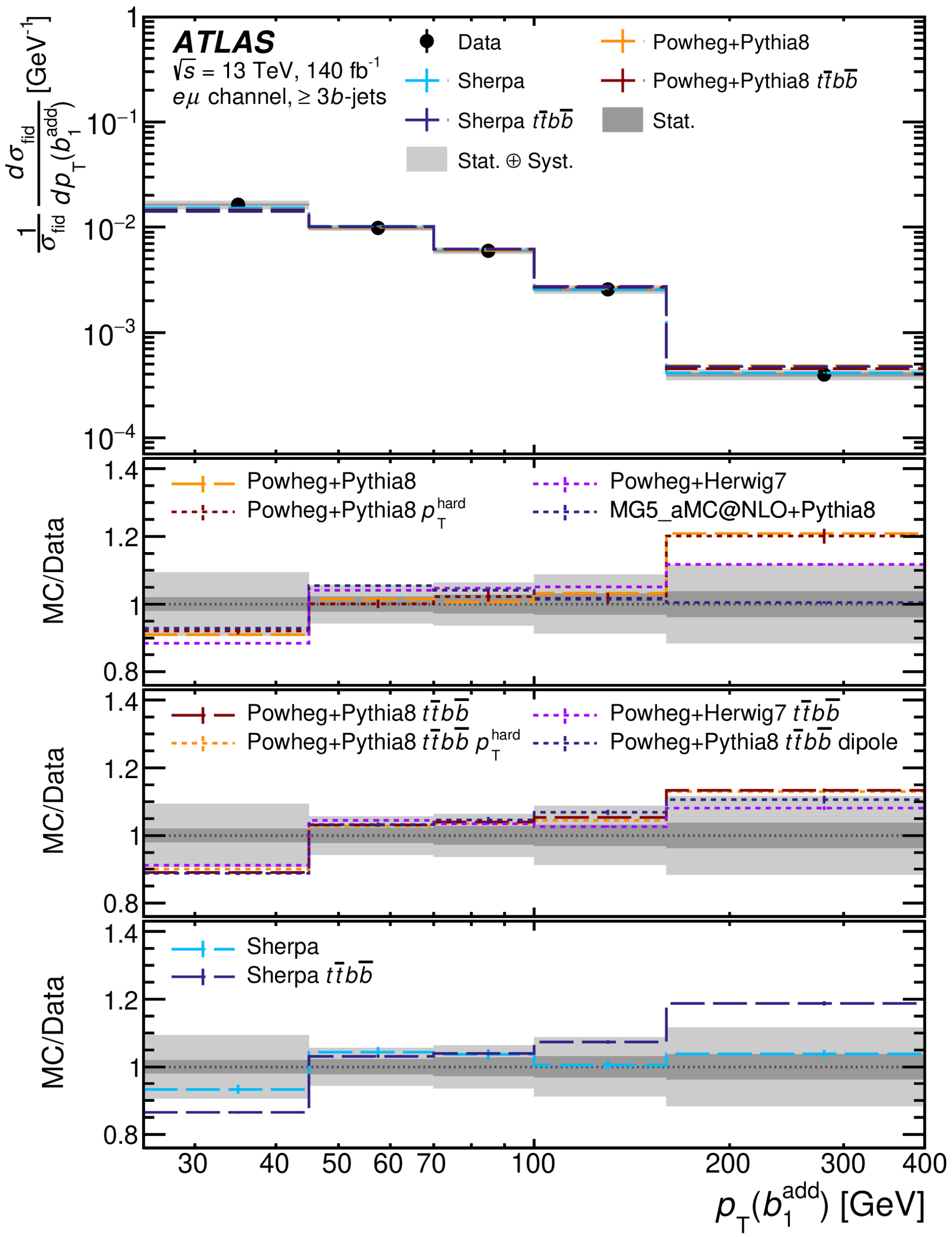

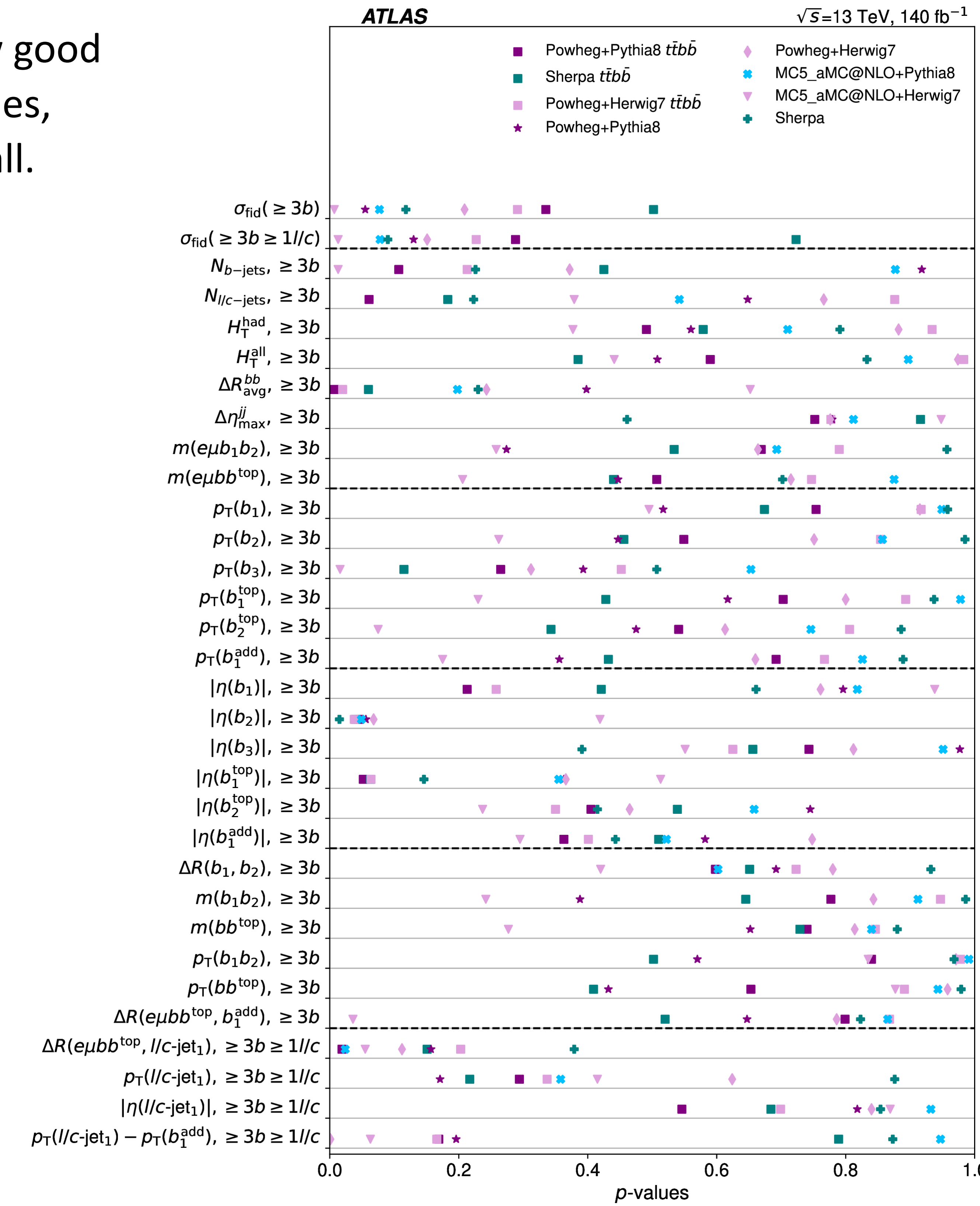

arXiv:2407.13473

Inclusive and differential cross section measurement of $t\bar{t}b\bar{b}$ production in the lepton+jets channel at $\sqrt{s} = 13\ \mathrm{TeV}$ [with the CMS detector]

JHEP 05 (2024) 042

Analysis Strategy

Particle level measurement in semi-leptonic e/μ channels with additional jets: JHEP 05 (2024) 042

- Integrated fiducial cross section of 5j3b (≥5 jets: ≥3b), 6j4b (≥6 jets: ≥4b), 6j3b3l (≥6 jets: ≥3b, ≥3 light), 7j4b3l (≥7 jets: ≥4b, ≥3 light) regions.
- Normalized differential cross-sections as a function of various variables in the 4 phase spaces.
    - Some observables in 6j4b are defined after assigning *b*-jets to the additional jets using kinematic information at the detector level (and using truth info on the particle level).

The data are unfolded to the particle level after subtracting the estimated background and correcting for the detector effects:

- Distributions are unfolded to the particle level through binned maximum likelihood fit.
- Simultaneous differential and inclusive cross section measurements for each observable.
- Simultaneous fit in two or three regions, signal- and background-enriched, to better constrain the background contributions.

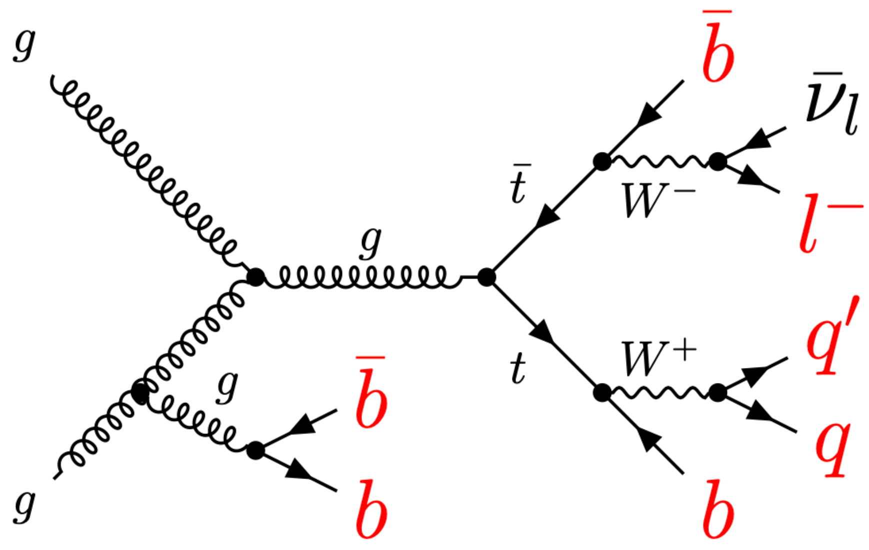

Ancillary Variable

In the selected regions with at least three *medium* $(75 - 80\,\%$ eff.) ***b*-tagged jets, the data are highly enriched in** $\mathrm{t\bar{t}}$**+jets events**, which consists of about $30\,\%$ $\mathrm{t\bar{t}B}$, $20\,\%$ $\mathrm{t\bar{t}C}$, and $50\,\%$ $\mathrm{t\bar{t}}$+light events.

The "ancillary" variable - the number of *tight* ($60\,\%$ efff.) *b*-jets - divides the detector-level selections into signal- and background-enriched categories, that are fitted simultaneously <u>to better constrain the background contribution</u>. The use of ancillary variables also constraints *b*-tagging uncertainties in the fit.

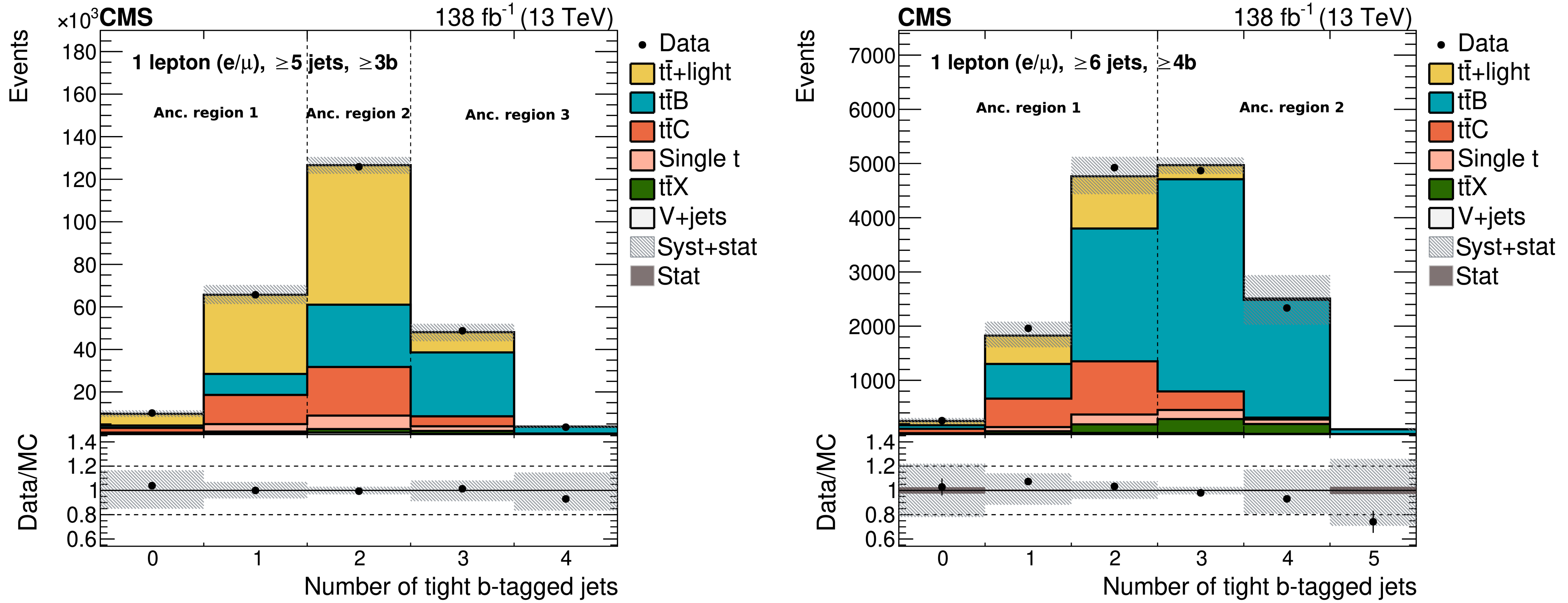

JHEP 05 (2024) 042

b-jets Origins Classification, Detector Level

8 observables in the 6j4b regions are related to physics with additional *b*-jets.

6 permutations of the 4 leading p_{T} *b*-jets (candidate jets) at the detector level are considered.

A DNN algorithm is trained with the candidate jets:

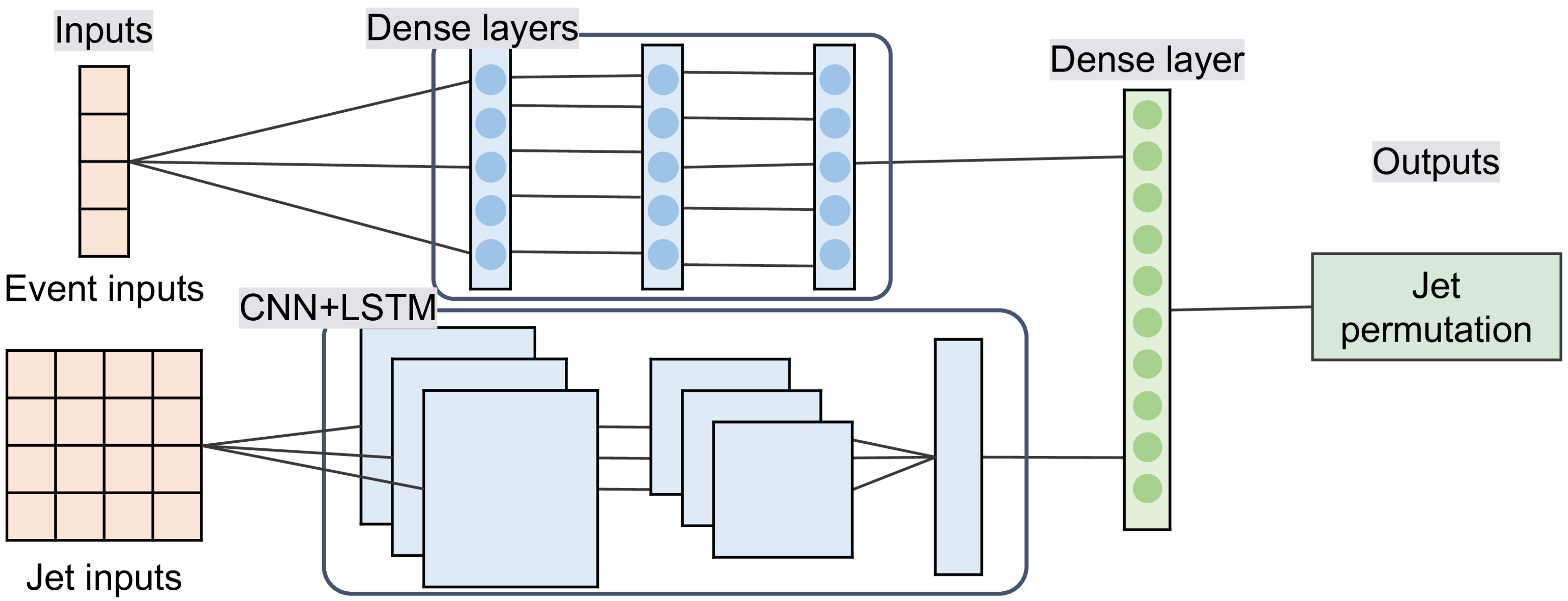

Jet inputs features are: p_{T} , η , *"is b-tight"* flag , $\Delta R(b, lep)$, $m_{\mathrm{inv}}(b, lep)$.

Event inputs features: 30 variables targeting global event information.

The pair of *b*-tagged jets with the highest DNN score per event is chosen as the additional *b*-jets.

The accuracy of the method is $\mathbf{49}$ % vs 41 % if selecting two closest in ΔR *b*-jets.

JHEP 05 (2024) 042

Fiducial Cross-Section Measurements: Results

Powheg+P8 $t\bar{t}b\bar{b}$ (4FS) is the only prediction which agrees well with the measurement in the 5j3b and overestimates cross sections in other phase spaces.

Powheg+P8 5FS with $\mu_{R/F} = m_T$ prediction agrees well in phase space with additional light jet radiation.

Other generators systematically under predict the cross sections compared to the measurements.

Measured and predicted fiducial cross-section results

JHEP 05 (2024) 042

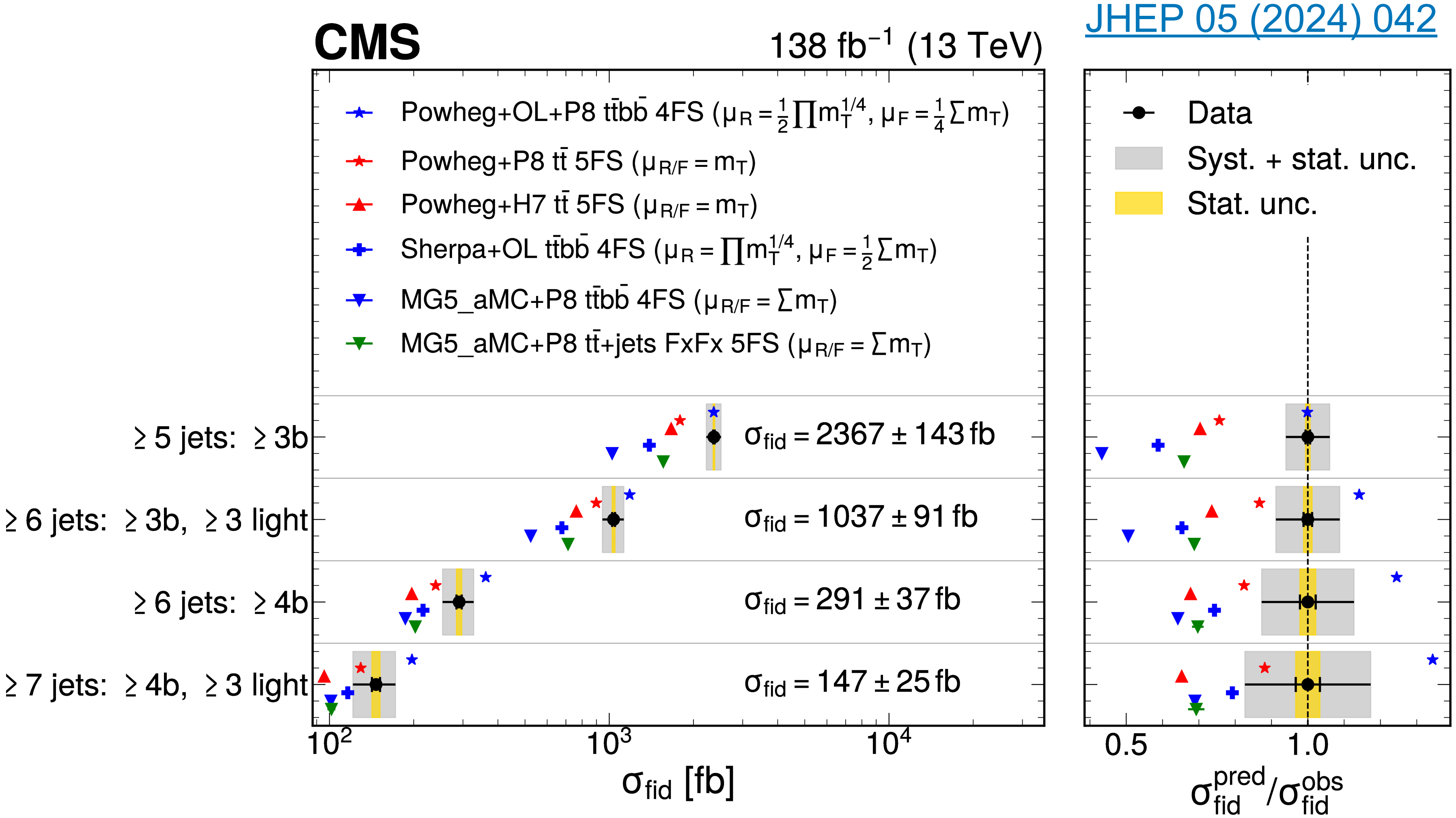

Overall, in all phase space regions, the measured cross sections are larger than the theoretical predictions except for Powheg+P8 $t\bar{t}b\bar{b}$ (4FS) which agrees with the measurement in 5j3b and overestimates in other regions.

Fiducial Cross-Section Measurements: Systs

	Relative uncertainty (%)			
Uncertainty source	5j3b	6j3b3l	6j4b	7j4b3l
Integrated luminosity	1.6	1.6	2.0	1.8
Pileup reweighting	0.2	0.8	0.4	0.5
Lepton and trigger	1.1	0.9	1.9	1.8
JES, JER	2.1	1.6	3.5	5.7
b tagging	4.5	3.9	7.0	9.1
μ_R and μ_F scales	2.8	6.8	8.2	12
Top quark p_T modelling	0.3	1.0	0.6	1.3
PDF	0.2	0.7	1.0	1.9
PS scales	2.8	2.7	2.4	1.5
ME-PS matching (h_{damp})	0.4	0.9	1.3	2.8
Underlying event	0.4	<0.1	0.4	0.4
Colour reconnection	1.1	1.5	1.9	4.5
b quark fragmentation	0.3	0.4	0.4	0.4
Inclusive $t\bar{t}C$ cross section	0.5	0.3	1.9	2.6
MC statistical	0.8	1.6	2.4	2.8
Total systematic uncertainty	6.0	8.7	13	17
Statistical uncertainty	0.6	1.2	2.2	3.3
Total uncertainty	6.0	8.8	13	17

JHEP 05 (2024) 042

Differential Cross-Section Measurements

Right: observed z score for each of the theoretical predictions. A lower value indicates a better agreement between prediction and measurement. The dashed line at $z = 2$ indicates $p-$value of $5\,\%$.

The agreement is generally better in the 6j4b phase space, at least in part due to the large uncertainties in the measurements.

Left: Example of unfolded distribution $\Delta R(bb^{extra})$

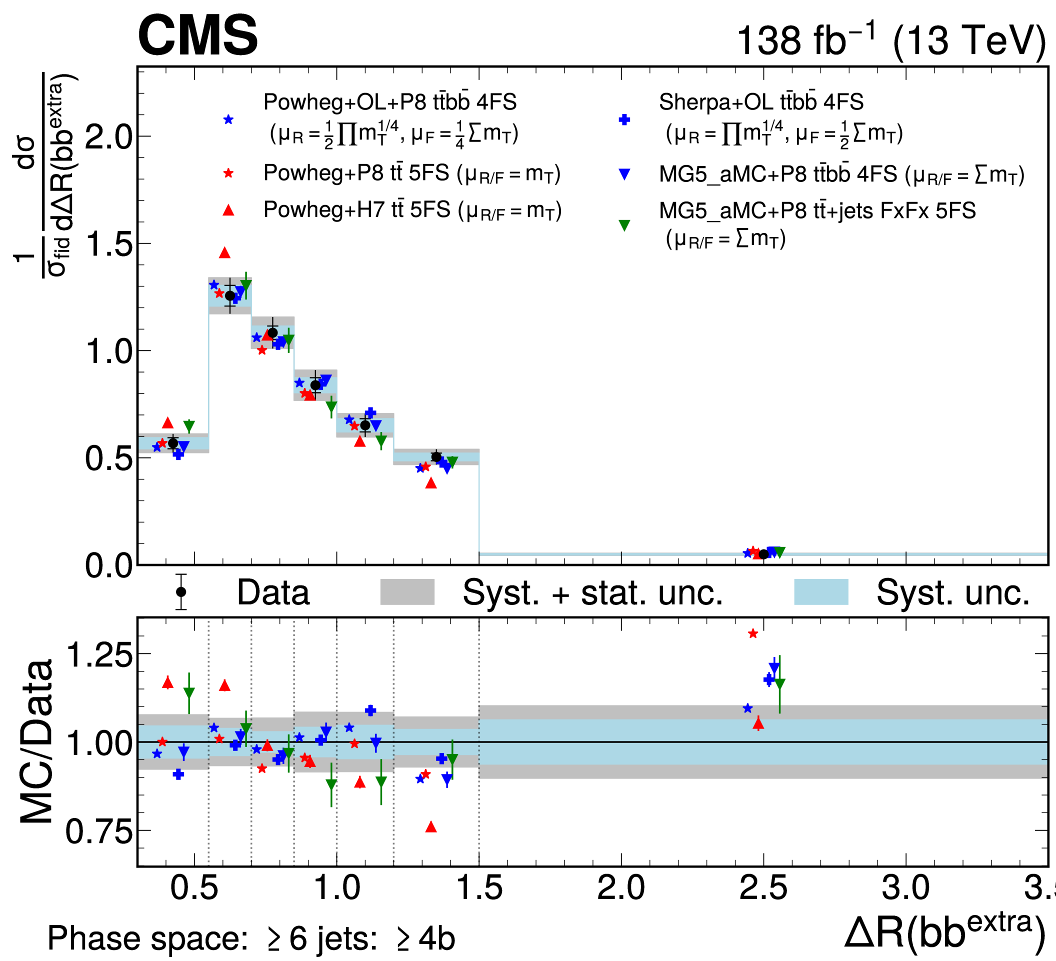

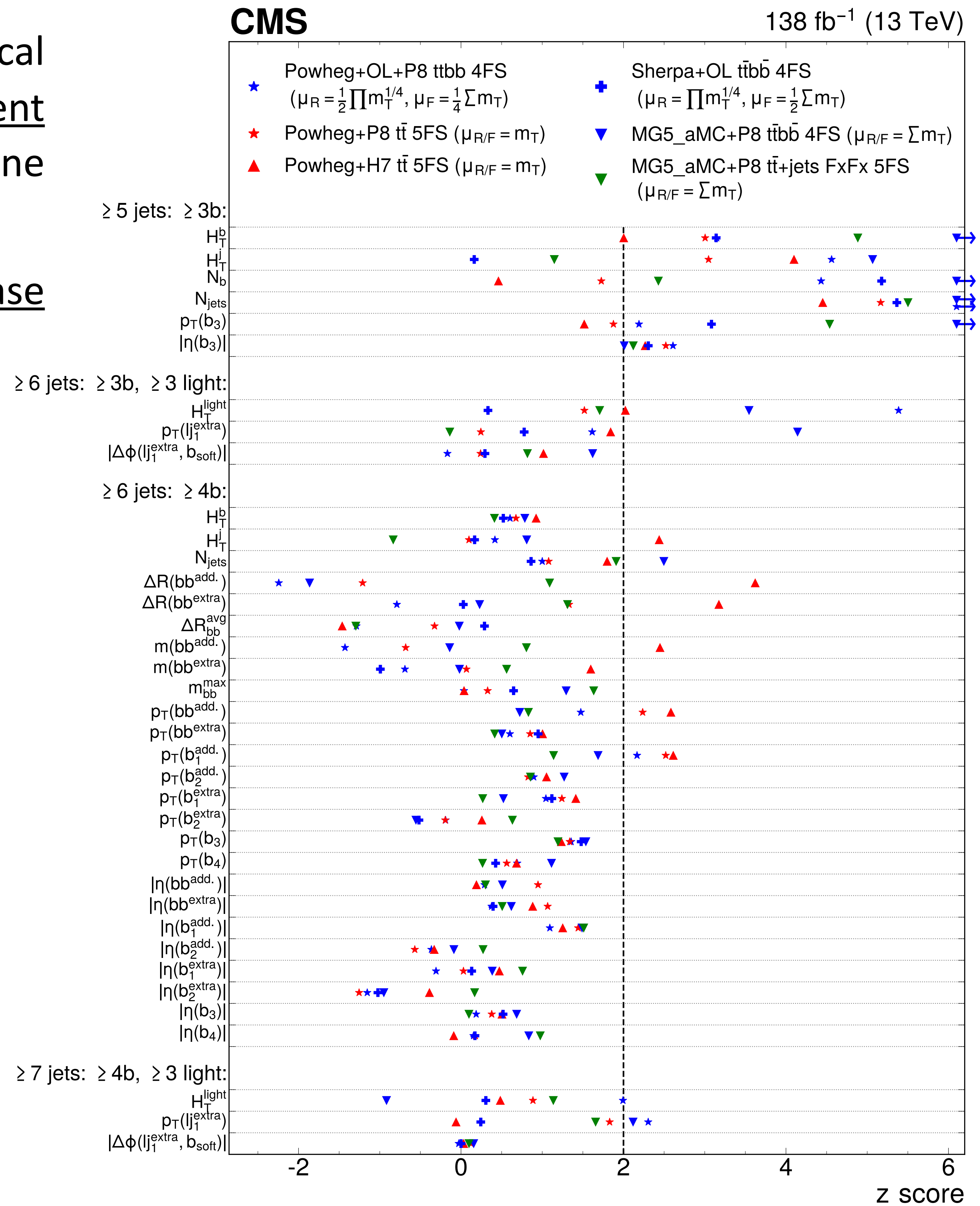

JHEP 05 (2024) 042

Summary

The ATLAS and CMS collaborations recently released measurements of $t\bar{t}b\bar{b}$ production with additional *b*-jets using full Run-2 LHC dataset. Both are the most up-to-date and most precise measurements of corresponding channels:

- ATLAS: $e\mu - OS$ channel with at least three and at least four *b*-jets at $\sqrt{s} = 13\ \mathrm{TeV},\ 140\ \mathrm{fb}^{-1}$:
    - The measured integrated cross-sections are consistent with $t\bar{t}b\bar{b}$ predictions from various NLO ME+PS calculations within the uncertainties of the predictions ($8.5 - 14.8\,\%$).
    - None of the predictions simultaneously describe all observables in differential measurements.
    - The leading uncertainties are systematic: *b*-tagging, jet energy scale and $t\bar{t}$ modeling.
- CMS: semi leptonic (e/μ) channel in 5j3b, 6j4b, 6j3b3l, 7j4b3l at $\sqrt{s} = 13\ \mathrm{TeV},\ 138\ \mathrm{fb}^{-1}$:
    - For most of the tested generators, the measured inclusive cross sections with total uncertainty of $6 - 17\,\%$ depending on a channel exceed the predictions.
    - None of the predictions simultaneously describe all observables in differential measurements.
    - The leading uncertainties are systematic: *b*-tagging, jet energy scale, choice of μ_r scale.

ATLAS EXPERIMENT

arXiv:2407.13473

CMS

JHEP 05 (2024) 042

Thank you!


top 2024
17th International Workshop on
Top Quark Physics
September 22 to 27
Saint-Malo, France

Backup

$t\bar{t}b\bar{b}$ Production Modes at the LHC

Top quark pair $t\bar{t}$ production governed by the strong interaction:

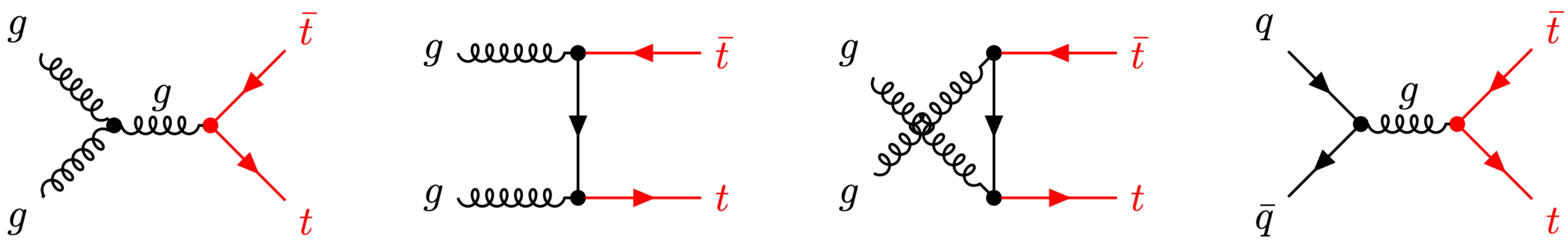

The final state topology is driven by:

- the *W*-bosons decays:

$(t \to Wb)$, $W \to l\nu(\sim 33\%)$ or $qq'(\sim 67\%)$

- ISR/FSR:

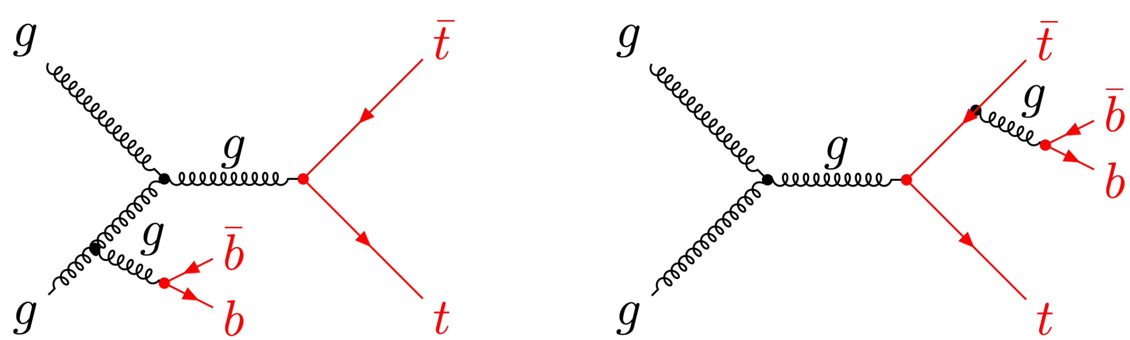

- Production mode:

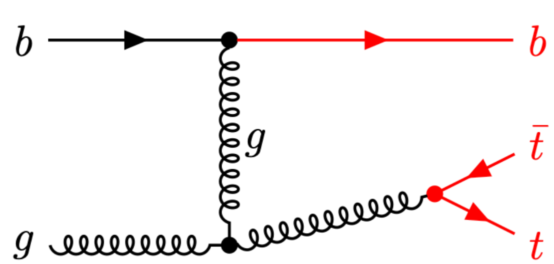

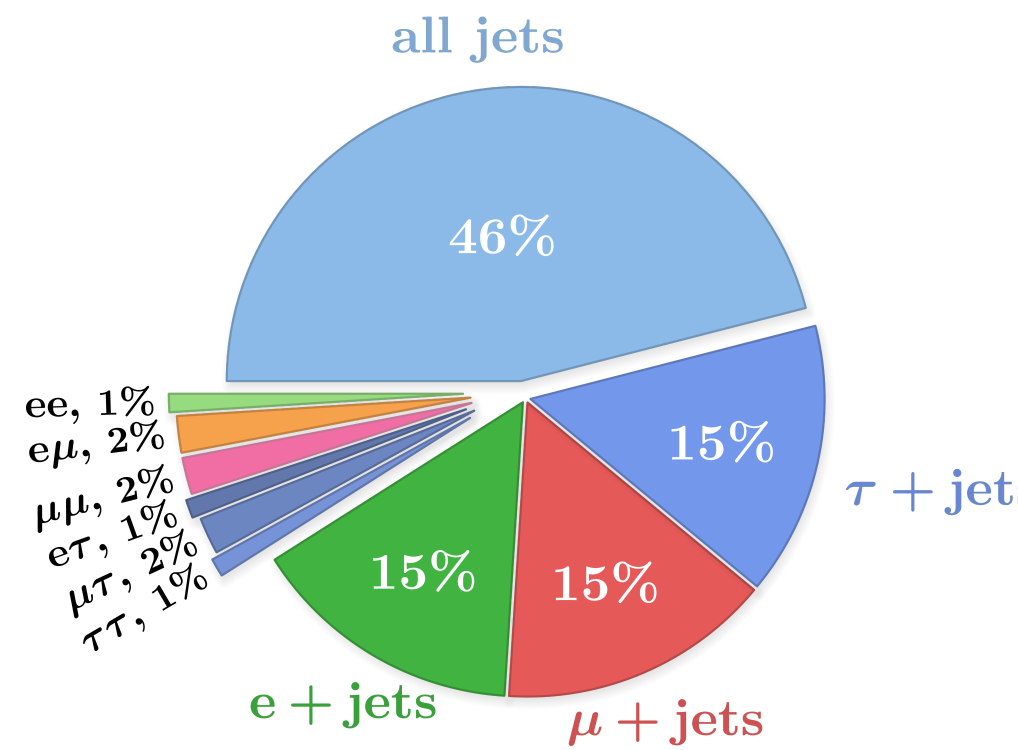

Top pair branching fractions

ATLAS and CMS $t\bar{t}b(\bar{b})$ Measurements

Before the full Run-2 analyses (discussed down in the talk), ATLAS and CMS measured cross-sections of $t\bar{t}$ pair with additional b-jets productions:

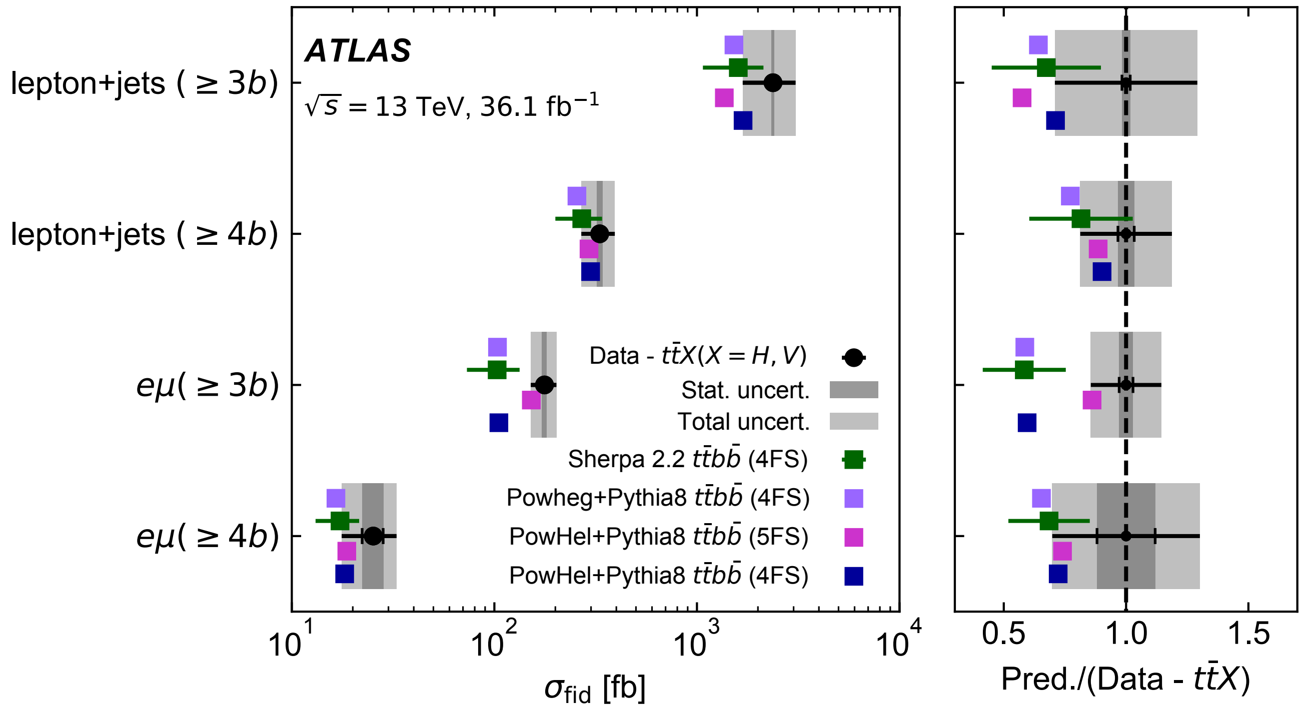

[JHEP 04 (2019) 046]

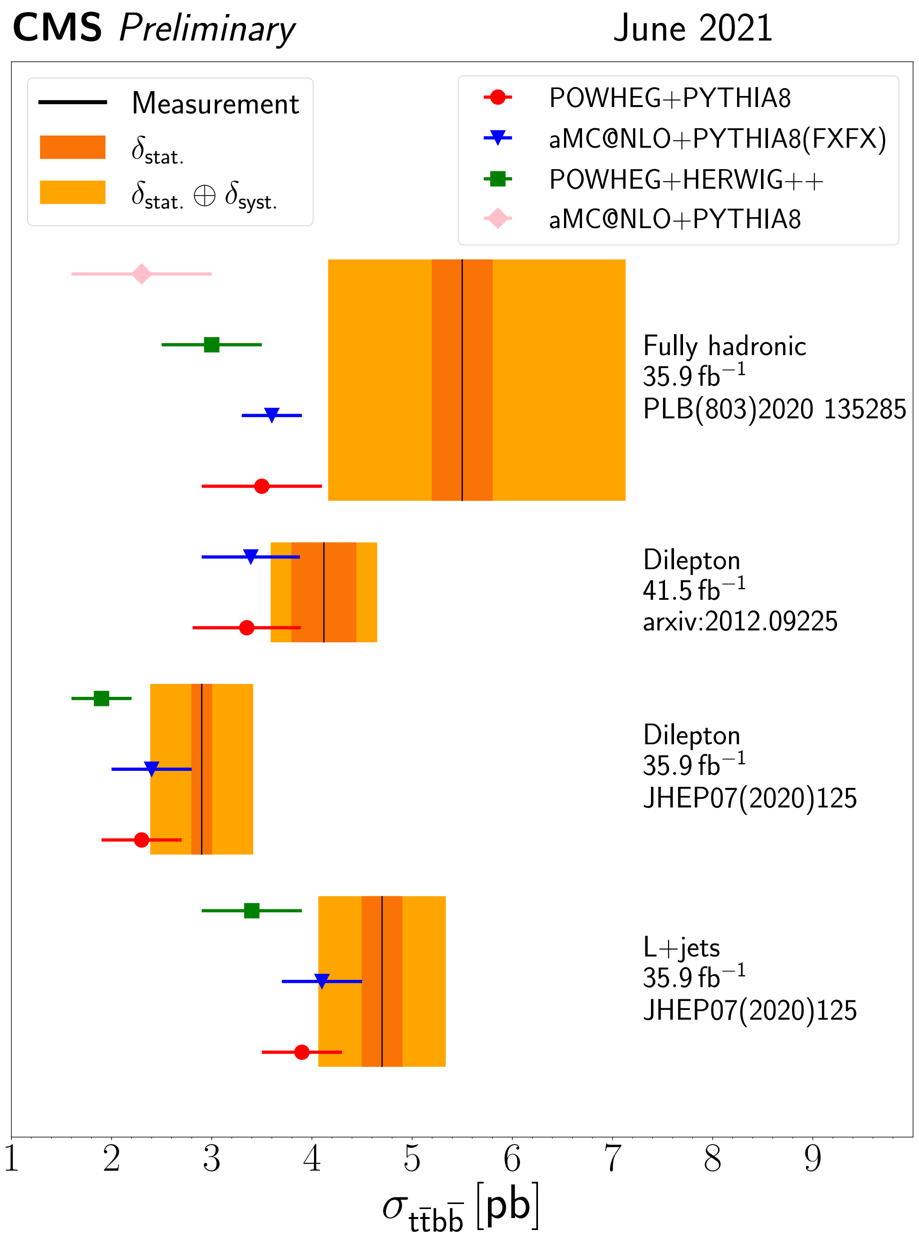

[CMS public results]

The ATLAS Detector

ATLAS consists of an inner tracking detector surrounded by a thin superconducting solenoid, electromagnetic and hadronic calorimeters, and a muon spectrometer incorporating three large superconducting air-core toroidal magnets.

- Inner detector:
  - silicon tracker (pixels + strips) $|\eta| < 2.5$;
  - transition radiation tracker with $|\eta| < 2.0$; also provides electrons identification info.
- Calorimeters:
  - hadronic and electromagnetic, $|\eta| < 4.9$.
- Muon spectrometer: $|\eta| < 2.7$.

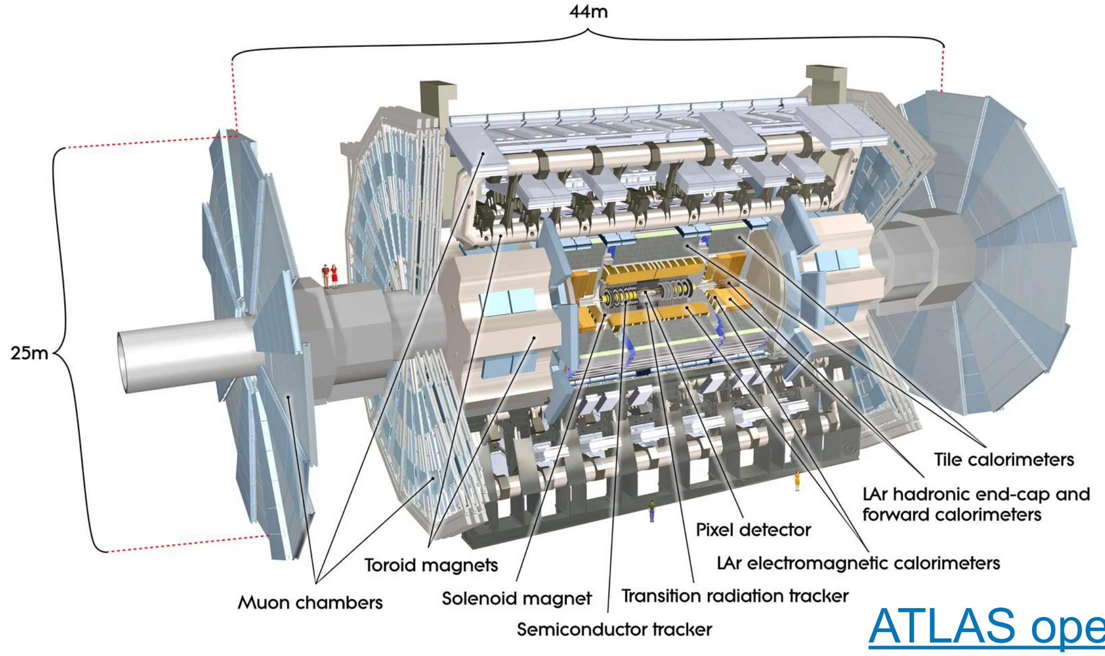

ATLAS open data

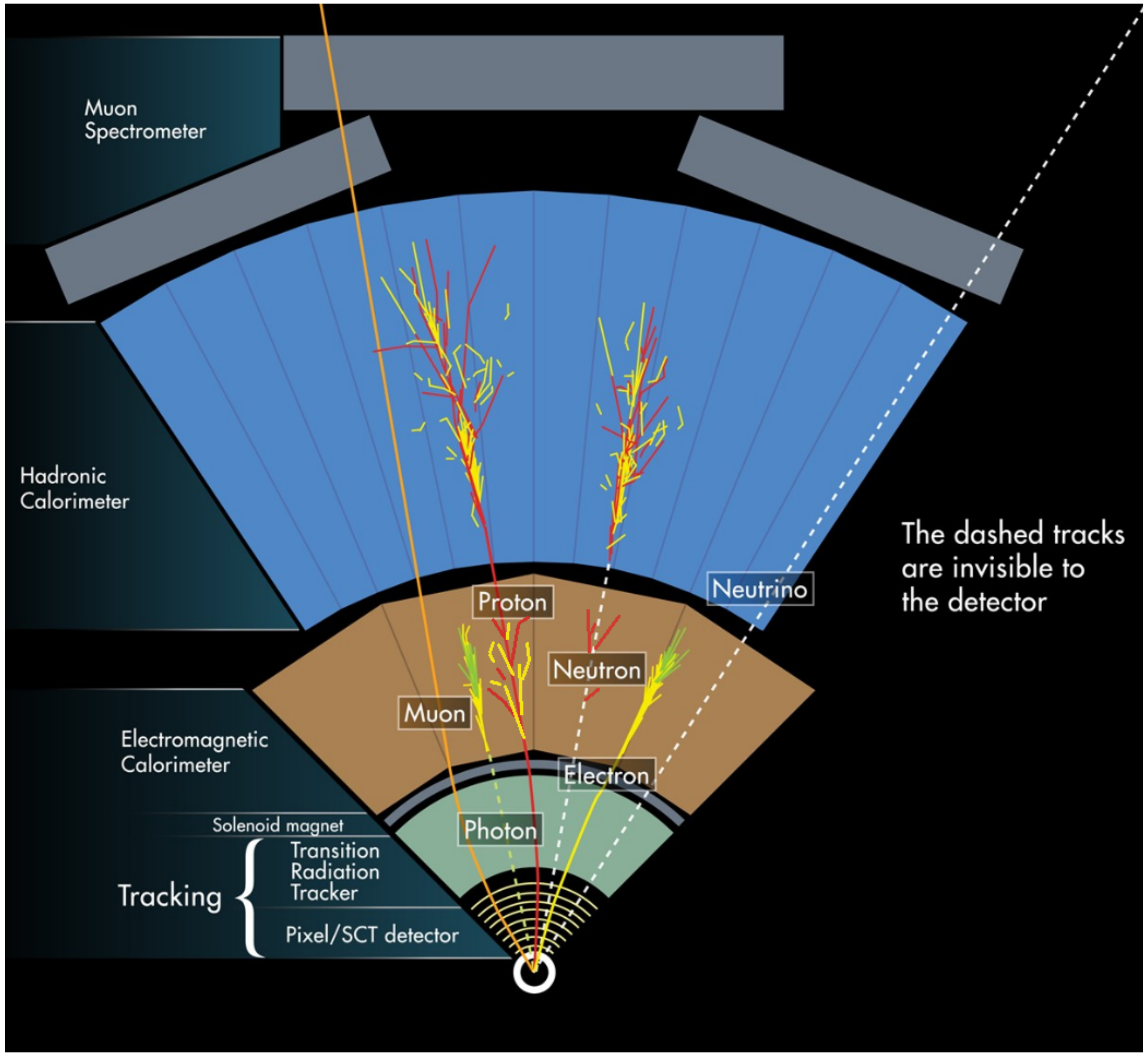

ATLAS-OUTREACH-2021-052

The CMS Detector

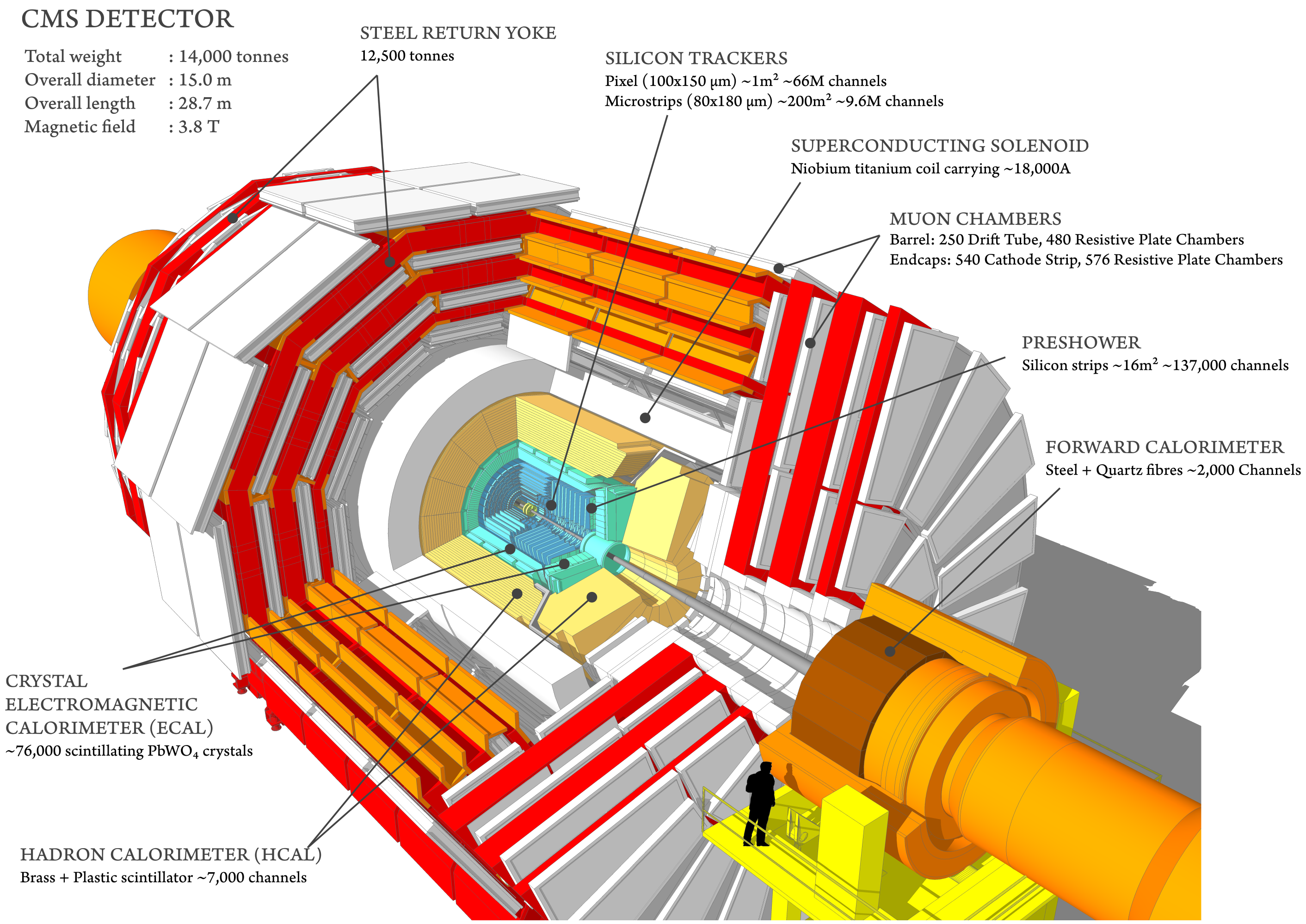

[CMS experiment webpage]

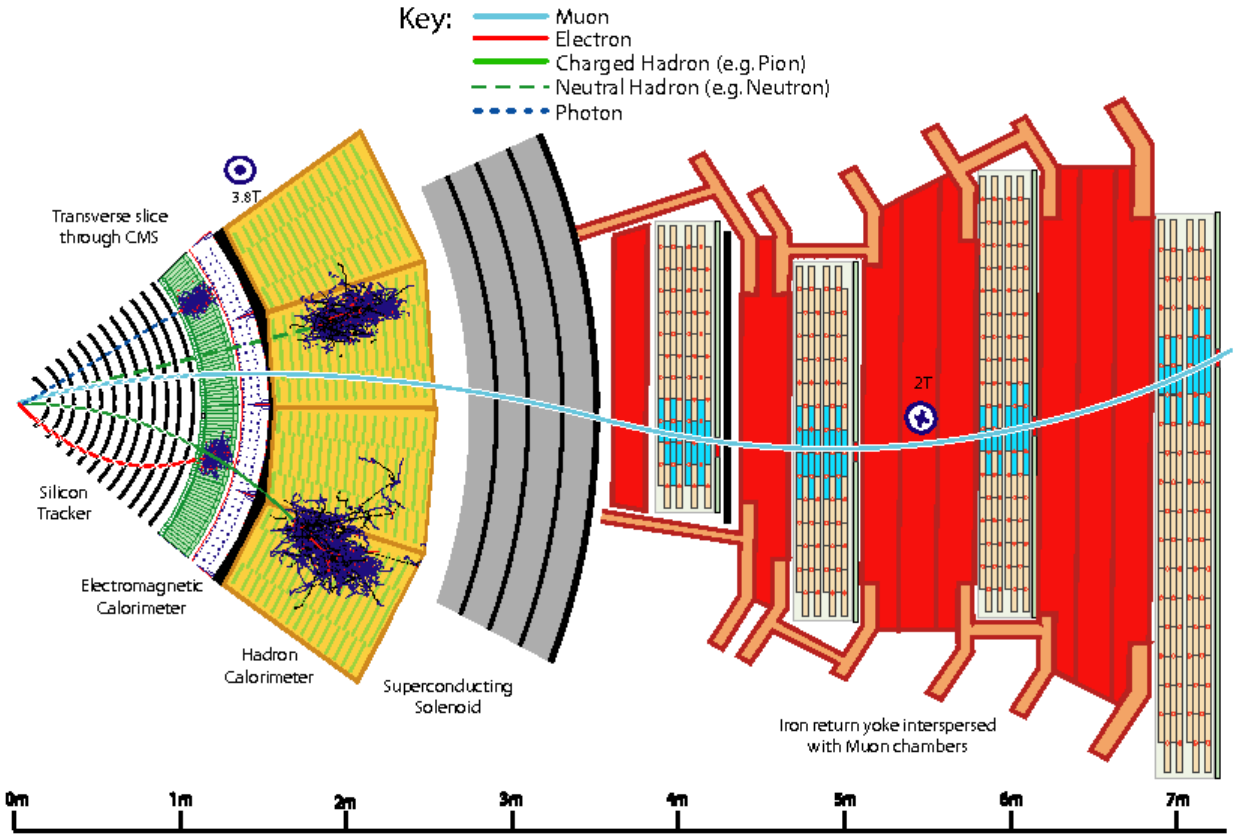

[arXiv:1706.04965]

$t\bar{t}$ Events candidates at ATLAS and CMS

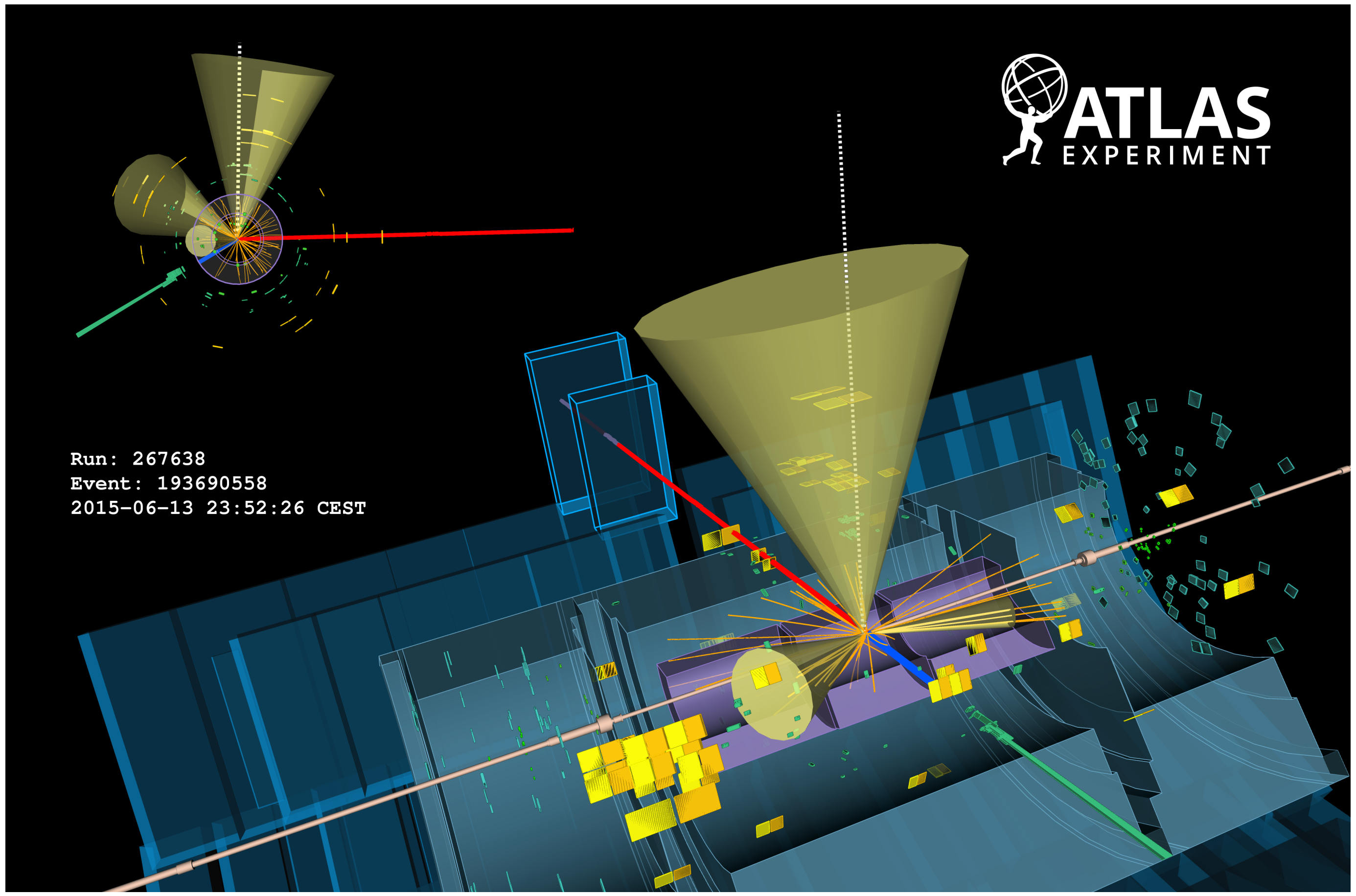

ATLAS $t\bar{t}$ event candidate with three jets (two b-tagged), an electron and a muon

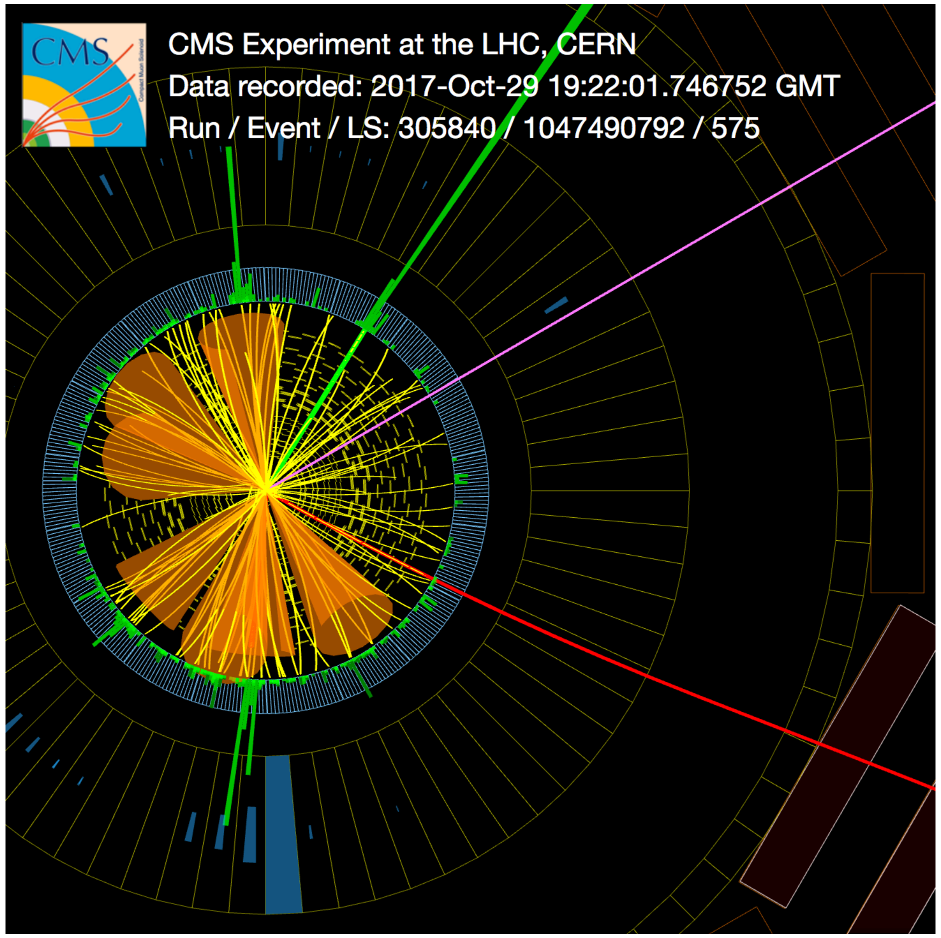

CMS $t\bar{t}b\bar{b}/t\bar{t}H$ event candidate with 7 jets (four b-tagged), an electron and a muon

ATLAS Signal Monte Carlo Samples

	MC sample	Generator	Process	Parton shower	Matching/ Parton shower settings	Tune	Use
Nominal	Powheg+Pythia8	Powheg Box v2	$t\bar{t}$ NLO	Pythia 8.230	Powheg h_{damp} =1.5m_{top} p_T^{hard} = 0 globalRecoil recoilToColoured=ON	A14	nom.
Systematics	Powheg+Pythia8 h_{damp}	Powheg Box v2	$t\bar{t}$ NLO	Pythia 8.230	Powheg h_{damp} =3m_{top}	A14	syst.
	Powheg+Pythia8 p_T^{hard}	Powheg Box v2	$t\bar{t}$ NLO	Pythia 8.230	Powheg p_T^{hard} = 1	A14	syst.
	Powheg+Pythia8 RecoilToTop	Powheg Box v2	$t\bar{t}$ NLO	Pythia 8.230	Powheg recoilToTop	A14	syst.
	Powheg+Herwig 7	Powheg Box v2	$t\bar{t}$ NLO	Herwig 7.1.3	Powheg	H7.1-Default	syst.
For comparison only (not systematics)	Powheg+Pythia8 dipole	Powheg Box v2	$t\bar{t}$ NLO	Pythia 8.230	Powheg dipoleRecoil on	A14	comp.
	MadGraph5_aMC@NLO+Pythia 8	MadGraph5_ aMC@NLO v2.6.0	$t\bar{t}$ NLO	Pythia 8.230	MC@NLO	A14	comp.
	MadGraph5_aMC@NLO+Herwig 7	MadGraph5_ aMC@NLO v2.6.0	$t\bar{t}$ NLO	Herwig 7.1.3	MC@NLO	H7.1-Default	comp.
	Sherpa	Sherpa 2.2.12	$t\bar{t}$ +0,1 parton at NLO +2,3,4 parton at LO	Sherpa	MePs@Nlo	Author's tune	comp.
	Powheg+Pythia8 $t\bar{t}b\bar{b}$	Powheg Box Res	$t\bar{t}b\bar{b}$ NLO	Pythia 8.230	Powheg Box Res h_{bzd}=5 p_T^{hard} = 0 globalRecoil	A14	comp.
	Powheg+Pythia8 $t\bar{t}b\bar{b}$ p_T^{hard}	Powheg Box Res	$t\bar{t}b\bar{b}$ NLO	Pythia 8.230	Powheg Box Res p_T^{hard} = 1	A14	comp.
	Powheg+Pythia8 $t\bar{t}b\bar{b}$ h_{bzd}	Powheg Box Res	$t\bar{t}b\bar{b}$ NLO	Pythia 8.230	Powheg Box Res h_{bzd}=2	A14	comp.
	Powheg+Pythia8 $t\bar{t}b\bar{b}$ dipole	Powheg Box Res	$t\bar{t}b\bar{b}$ NLO	Pythia 8.230	Powheg Box Res h_{bzd}=2 dipoleRecoil on	A14	comp.
	Powheg+Herwig 7 $t\bar{t}b\bar{b}$	Powheg Box Res	$t\bar{t}b\bar{b}$ NLO	Herwig 7.1.6	Powheg Box Res	H7.1-Default	comp.
	Sherpa $t\bar{t}b\bar{b}$	Sherpa 2.2.10	$t\bar{t}b\bar{b}$ NLO	Sherpa	MePs@Nlo	Author's tune	comp.
	Helac-NLO (off-shell)	Helac-NLO	$e\mu + 4b$ NLO	–	–	–	comp.

arXiv:2407.13473

ATLAS $t\bar{t}b\bar{b}$: Observables

summary of all measured observable in each fiducial phase space region

arXiv:2407.13473

Observable	Description	Phase spaces ≥ 2b	≥ 3b	≥ 3b ≥ 1light	≥ 4b	≥ 4b ≥ 1light
σ^{fid}	Fiducial total cross-section		✓	✓	✓	✓
$N_{b\text{-jets}}$	Number of b-jets	✓	✓			
$N_{\text{light jets}}$	Number of light jets		✓		✓	
H_T^{had}	Scalar sum of p_T of all jets		✓		✓	
H_T^{all}	Scalar sum of p_T of charged leptons, jet and missing E_T		✓		✓	
$\Delta R_{\text{avg}}^{bb}$	Average angular distance in ΔR of b-jets pairs		✓		✓	
$\Delta\eta_{\text{max}}^{jj}$	Maximum absolute difference in η between any pair of jets		✓		✓	
$p_T\ (b_1)$	p_T of the hardest b-jet		✓		✓	
$p_T\ (b_2)$	p_T of second-hardest b-jet		✓		✓	
$p_T\ (b_3)$	p_T of third-hardest b-jet		✓		✓	
$p_T\ (b_4)$	p_T of fourth-hardest b-jet				✓	
$\eta(b_1)$	η of hardest b-jet		✓		✓	
$\eta(b_2)$	η of second-hardest b-jet		✓		✓	
$\eta(b_3)$	η of third-hardest b-jet		✓		✓	
$\eta(b_4)$	η of fourth-hardest b-jet				✓	
$p_T\ (\text{light jet}_1)$	p_T of the hardest light jet			✓		✓
$\eta(\text{light jet}_1)$	η of the hardest light jet			✓		✓
$m(b_1b_2)$	Invariant mass of two hardest b-jets in p_T		✓		✓	
$\Delta R(b_1, b_2)$	ΔR between two hardest b-jets		✓		✓	
$p_T\ (b_1b_2)$	p_T of two hardest b-jets		✓		✓	
$m(bb^{\min\Delta R})$	Invariant mass of two closest b-jets in ΔR				✓	
$p_T(bb^{\min\Delta R})$	p_T of the closest b-jets pair				✓	
$\min\Delta R(bb)$	Closest angular distance in ΔR among b-jets				✓	
$m(e\mu b_1b_2)$	Invariant mass of electron, muon and two hardest b-jets		✓		✓	
$p_T\ (b_1^{\text{top}})$	p_T of the hardest b-jet assigned to top quark		✓		✓	
$p_T\ (b_2^{\text{top}})$	p_T of the second-hardest b-jet assigned to top quark		✓		✓	
$p_T\ (b_1^{\text{add}})$	p_T of the hardest additional b-jet		✓		✓	
$p_T\ (b_2^{\text{add}})$	p_T of the second-hardest additional b-jet				✓	
$\eta(b_1^{\text{top}})$	η of the hardest b-jet assigned to top quark		✓		✓	
$\eta(b_2^{\text{top}})$	η of the second-hardest b-jet assigned to top quark		✓		✓	
$\eta(b_1^{\text{add}})$	η of the hardest additional b-jet		✓		✓	
$\eta(b_2^{\text{add}})$	η of the second-hardest additional b-jet				✓	
$m(bb^{\text{top}})$	Invariant mass of a pair of b-jets assigned to top quarks		✓		✓	
$p_T\ (bb^{\text{top}})$	p_T of a pair of b-jets assigned to top quarks		✓		✓	
$m(bb^{\text{add}})$	Invariant mass of a pair of additional b-jets				✓	
$p_T\ (bb^{\text{add}})$	p_T of a pair of additional b-jets				✓	
$m(e\mu bb^{\text{top}})$	Invariant mass of $e\mu$ and the b-jets pair assigned to top quarks		✓		✓	
$\Delta R(e\mu bb^{\text{top}}, b_1^{\text{add}})$	ΔR between the direction of the system of $e\mu$ and b-jets pair assigned to top and the direction of the hardest additional b-jet		✓		✓	
$\Delta R(e\mu bb^{\text{top}}, \text{light jet}_1)$	ΔR between the direction of the system of $e\mu$ and b-jets pair assigned to tops and the direction of the hardest light-flavored jet			✓		✓
$p_T\ (\text{light jet}_1) - p_T(b_1^{\text{add}})$	Difference in p_T of the hardest light jet and the additional b-jet			✓		✓

ATLAS Objects and Event Selection

	$t\bar{t}$ +b-jets		
	$t\bar{t}$ +$\geq 0b$	$t\bar{t}$ +$\geq 1b$	$t\bar{t}$ +$\geq 2b$
Electron	$p_T > 28$ GeV $\|\eta\| < 2.5$		
Muon	$p_T > 28$ GeV $\|\eta\| < 2.5$		
jets/b-jets	$p_T > 25$ GeV $\|\eta\| < 2.5$		
Number of electron (N_e)	1		
Number of muon (N_μ)	1		
Number of b-jets (N_b)	≥ 2	≥ 3	≥ 4
charge $Q_e + Q_\mu$	0		
ΔR(lepton, jet)	> 0.4		
e/μ from τ lepton decay	included		

arXiv:2407.13473

ATLAS $t\bar{t}$+jets Flavors Fit: Resulting Fit Values

arXiv:2407.13473

	Inclusive region *Global* approach	Regions in terms of jet multiplicity and third-highest-p_T jet-p_T *Kinematic-dependent* approach					
	(nominal)	(systematic)					
Category	$\geq 3j \geq 2b$@77% $\geq$ 25 GeV	$3j \geq 2b$@77% 25–35 GeV	35–50 GeV	$\geq$ 50 GeV	$\geq 4j \geq 2b$@77% 25–50 GeV	50–75 GeV	$\geq$ 75 GeV
$t\bar{t}b$	$\geq$3 b-jets	$\geq$3 b-jets			–		
$t\bar{t}b_{\text{ex}}$	–	–			exactly 3 b-jets		
$t\bar{t}b\bar{b}$	–	–			$\geq$4 b-jets		
$t\bar{t}c$	< 3 b-jets and ≥ 1 c-jet	< 3 b-jets and ≥ 1 c-jet			< 3 b-jets and ≥ 1 c-jet		
$t\bar{t}l$	events that do not meet above criteria	events that do not meet above criteria			events that do not meet above criteria		

Truth categorizations, defined using particle level information of the reconstructed events.

Best fit values of the scale factors determined from dedicated fit regions. The quoted uncertainties are statistical only.

Regions	Fitted values of scale factors α_b^s	$\alpha_{b\text{ex}}^s$	α_{bb}^s	α_c^s	α_l^s	Type
$\geq 3j \geq 2b$; $\geq$ 25 GeV	1.20 ± 0.03	–	–	1.62 ± 0.09	0.92 ± 0.04	*Global*
$3j \geq 2b$; (25–35) GeV	1.40 ± 0.15	–	–	1.99 ± 0.42	0.98 ± 0.08	*Kinematic-dependent*
$3j \geq 2b$; (35–50) GeV	1.30 ± 0.11	–	–	1.74 ± 0.27	0.77 ± 0.11	
$3j \geq 2b$; $\geq$ 50 GeV	1.26 ± 0.12	–	–	1.05 ± 0.27	1.09 ± 0.15	
$\geq 4j \geq 2b$; (25–50) GeV	–	1.31 ± 0.10	1.15 ± 0.14	1.93 ± 0.11	0.92 ± 0.01	
$\geq 4j \geq 2b$; (50–75) GeV	–	1.10 ± 0.09	1.20 ± 0.10	1.64 ± 0.09	0.86 ± 0.01	
$\geq 4j \geq 2b$; $\geq$ 75 GeV	–	1.10 ± 0.10	1.09 ± 0.10	1.25 ± 0.10	0.83 ± 0.02	

$$\nu_k(\alpha_b^s, \alpha_c^s, \alpha_l^s) = \alpha_b^s N_{t\bar{t}b}^{k,s} + \alpha_c^s N_{t\bar{t}c}^{k,s} + \alpha_l^s N_{t\bar{t}l}^{k,s} + N_{\text{non-}t\bar{t}}^{k,s}$$

$$\nu_k(\alpha_{b_{\text{ex}}}^s, \alpha_{bb}^s, \alpha_c^s, \alpha_l^s) = \alpha_{b\text{ex}}^s N_{t\bar{t}b_{\text{ex}}}^{k,s} + \alpha_{bb}^s N_{t\bar{t}b\bar{b}}^{k,s} + \alpha_c^s N_{t\bar{t}c}^{k,s} + \alpha_l^s N_{t\bar{t}l}^{k,s} + N_{\text{non-}t\bar{t}}^{k,s}$$

The expected number of events in k^{th} bin in ==3b (top) and ≥4b (bottom) regions

ATLAS $t\bar{t}$+jets Flavors Fit: *b*-tagging discriminant score distributions

Comparison of data and predictions for the *b*-tagging discriminant score distributions:

a: the inclusive 3j2b region considered for the *Global* fit.

b, c: the exclusive 3j2b region for two slices in the 3^{rd} *b*-tag score ranked p_{T} considered for the *Kinematic-dependent* fit.

d: the inclusive 4j2b for one slice in the 3^{rd} *b*-tag score ranked p_{T} considered for the *Kinematic-dependent* fit.

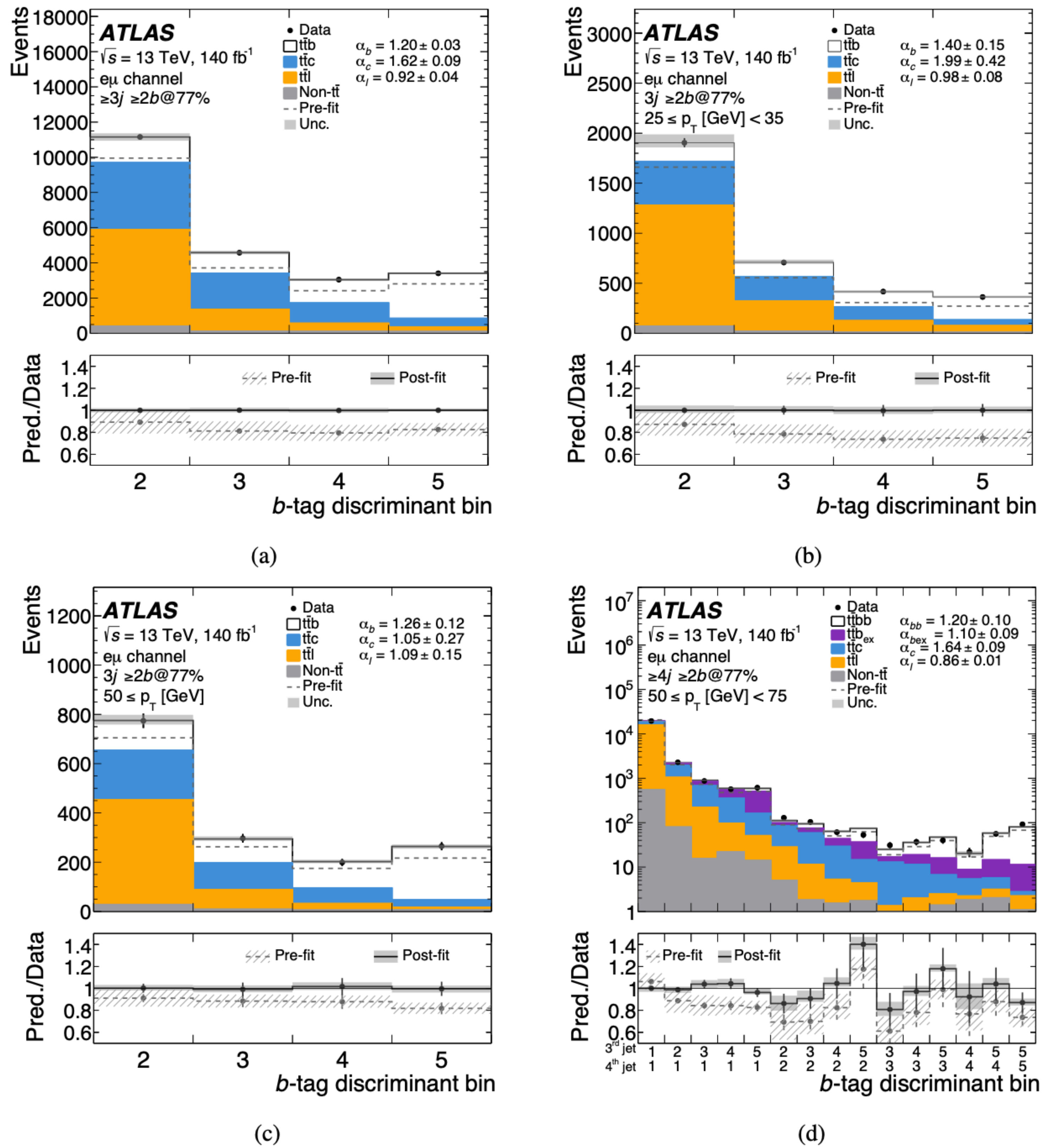

arXiv:2407.13473

ATLAS $t\bar{t}$+jets Flavors Fit: Compare Pre/Post

Left: pre-fit distributions for various variables of the analysis. Right: post-fit.

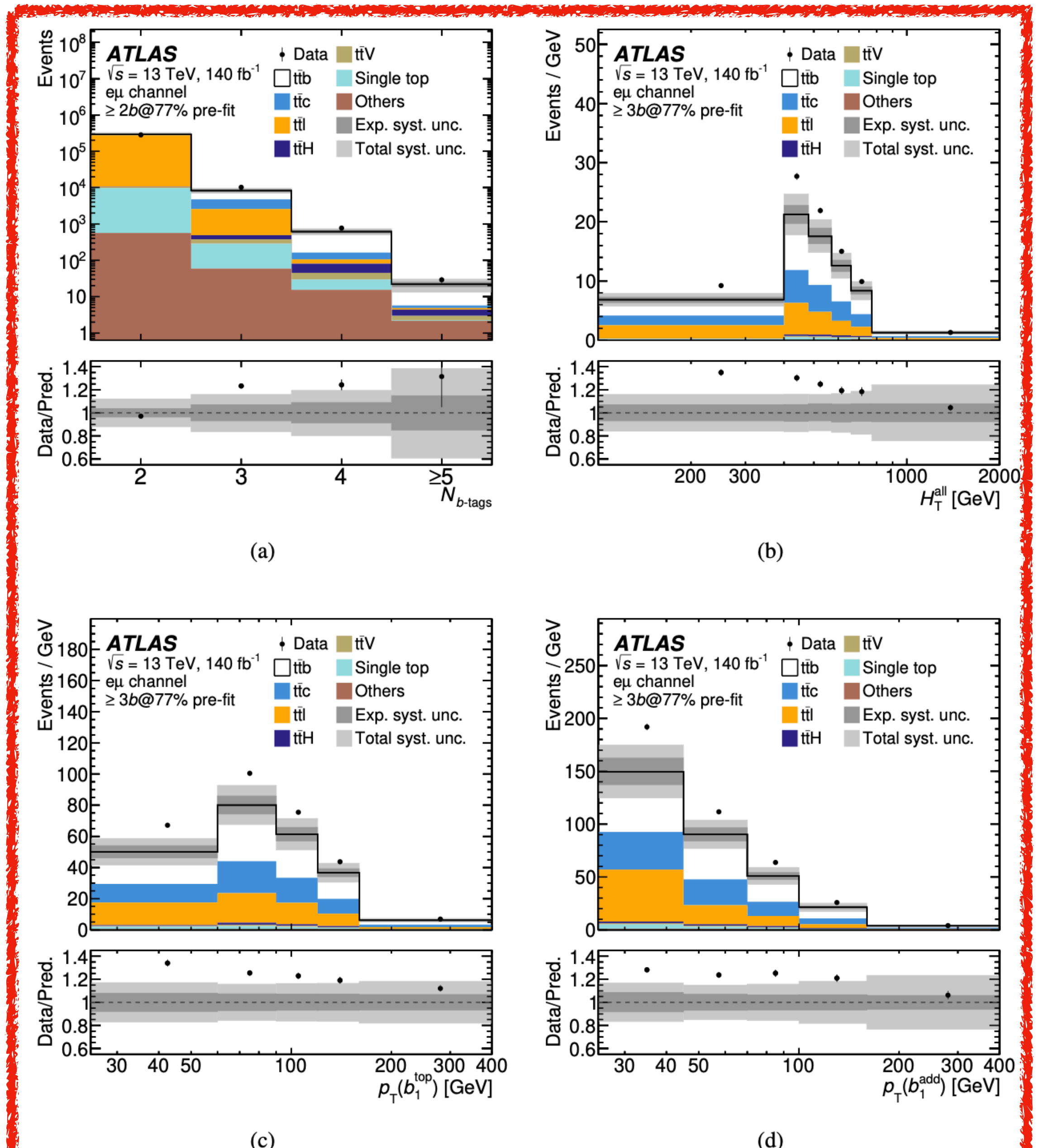

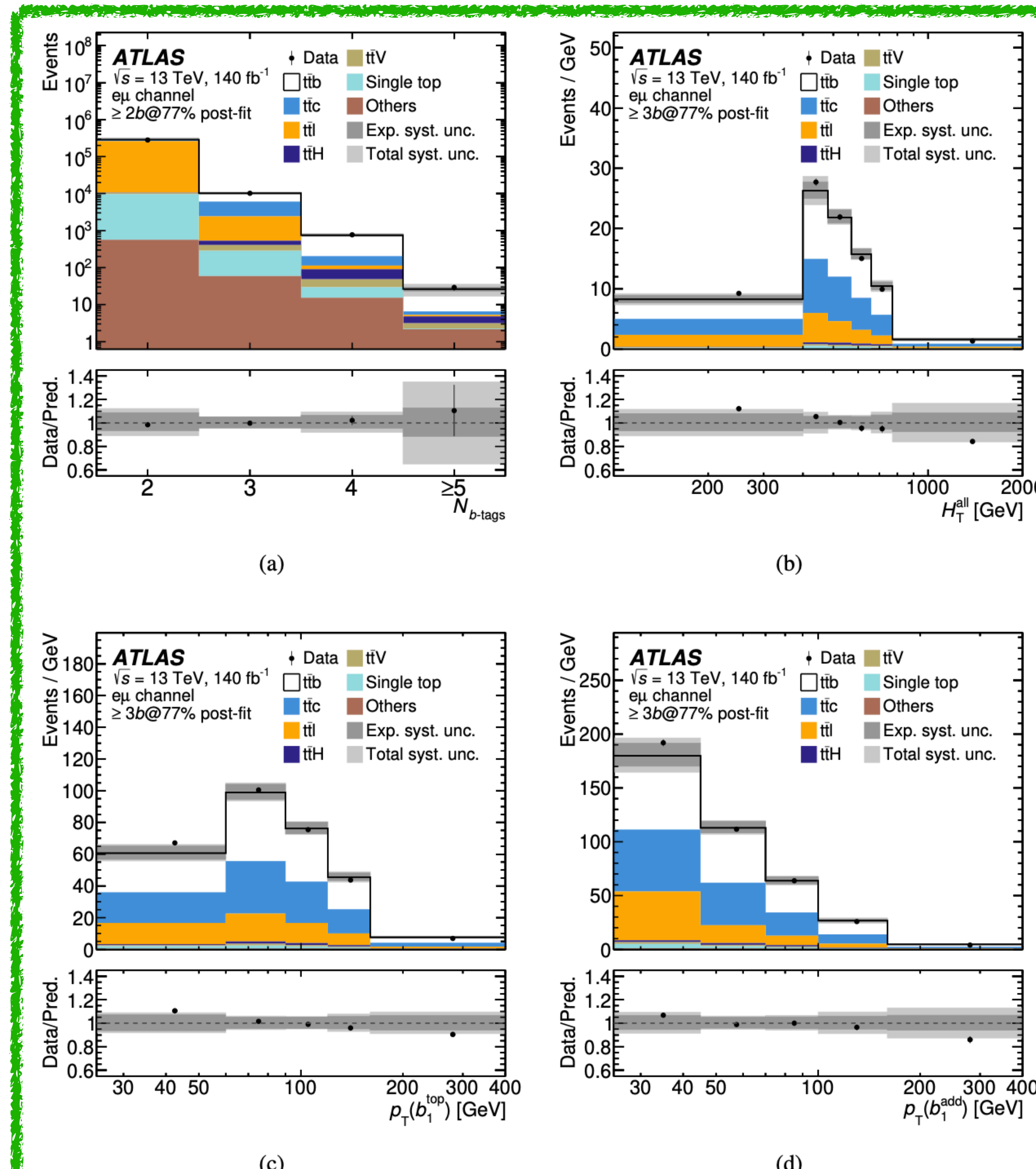

The data are described much better by the prediction after the individual $t\bar{t}j$ components are corrected.

arXiv:2407.13473

ATLAS Fake Leptons Background Estimation

Fake leptons background is a very small background in the analysis. arXiv:2407.13473

Data-driven estimation from fake dominated same-sign region:

$$N_{i,\mathrm{fake}} = R \cdot (N^{\mathrm{Data}}_{i,\mathrm{SS}} - N^{\mathrm{MC}}_{i,\mathrm{SS-prompt}}) \qquad R = \frac{N^{\mathrm{MC}}_{\mathrm{OS-non-prompt}}}{N^{\mathrm{MC}}_{\mathrm{SS-non-prompt}}}$$

Fake SS→OS scaling factors *R* are derived as a function of lepton p_T in events with at least two *b*-jets, and evaluated inclusively in lepton p_T in events with ≥3 b-jets.

The values of *R* range from 1.98 ± 0.52 to 2.38 ± 0.74 across the lepton-p_T bins in 2*b*@77% events, while it is 1.65 ± 0.45 for the inclusive ≥3*b*@77% events, where the quoted error represents the uncertainty due to limited MC statistics and the MC modeling uncertainty, with the latter being the dominant component.

ATLAS Fiducial Cross-Section Measurements: Results

Fiducial phase space	Fiducial cross-sections [fb] $\geq 3b$	$\geq 3b \geq 1l/c$	$\geq 4b$	$\geq 4b \geq 1l/c$
Measured	143 ±1 (stat) ±12 (syst)	87 ±1 (stat) ±8 (syst)	22 ±1 (stat) ±3 (syst)	14 ±1 (stat) ±2 (syst)
Powheg+Pythia 8 $t\bar{t}b\bar{b}$ (4FS)	132	78	23	14
Powheg+Pythia 8 $t\bar{t}b\bar{b}$ h_{bzd} (4FS)	129	74	21	13
Powheg+Pythia 8 $t\bar{t}b\bar{b}$ dipole (4FS)	128	71	22	13
Powheg+Pythia 8 $t\bar{t}b\bar{b}$ $p_{\mathrm{T}}^{\mathrm{hard}}$ (4FS)	129	68	21	12
Powheg+Herwig 7 $t\bar{t}b\bar{b}$ (4FS)	130	77	22	14
Sherpa $t\bar{t}b\bar{b}$ (4FS)	135	90	21	15
Helac-NLO (off-shell) $e\mu + 4b$	–	–	20	–
Powheg+Pythia 8 $t\bar{t}$ (5FS)	120	74	18	11
Powheg+Herwig 7 $t\bar{t}$ (5FS)	128	75	18	11
MG5_aMC@NLO+Pythia8 $t\bar{t}$ (5FS)	122	72	18	11
MadGraph5_aMC@NLO+Herwig 7 $t\bar{t}$ (5FS)	110	66	13	8
Sherpa 2.2.12 $t\bar{t}$ (5FS)	124	73	16	10

arXiv:2407.13473

Quantitative comparisons with predictions show good agreement for *most* observables within the measurement uncertainties, and the differences among various predictions are small.

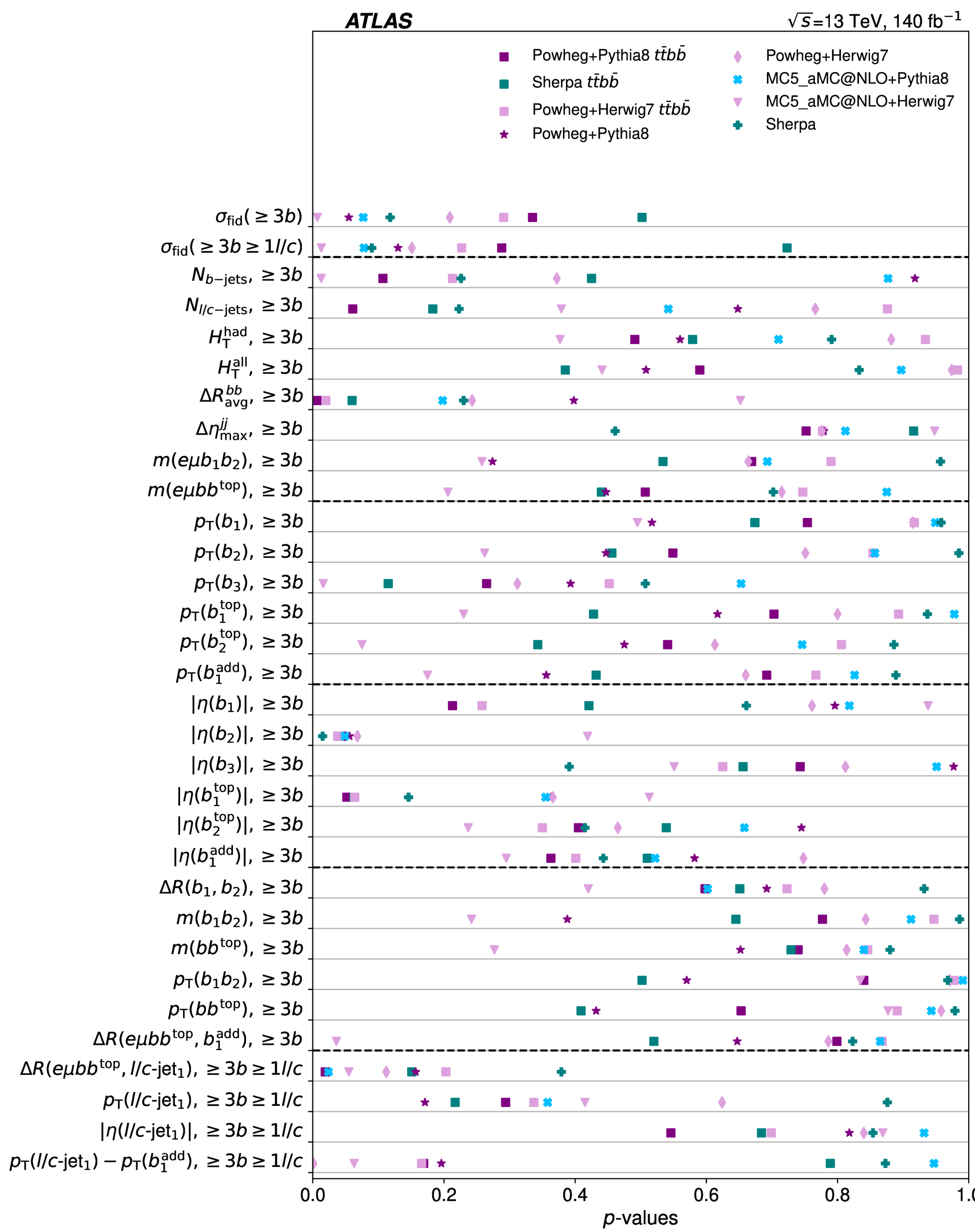

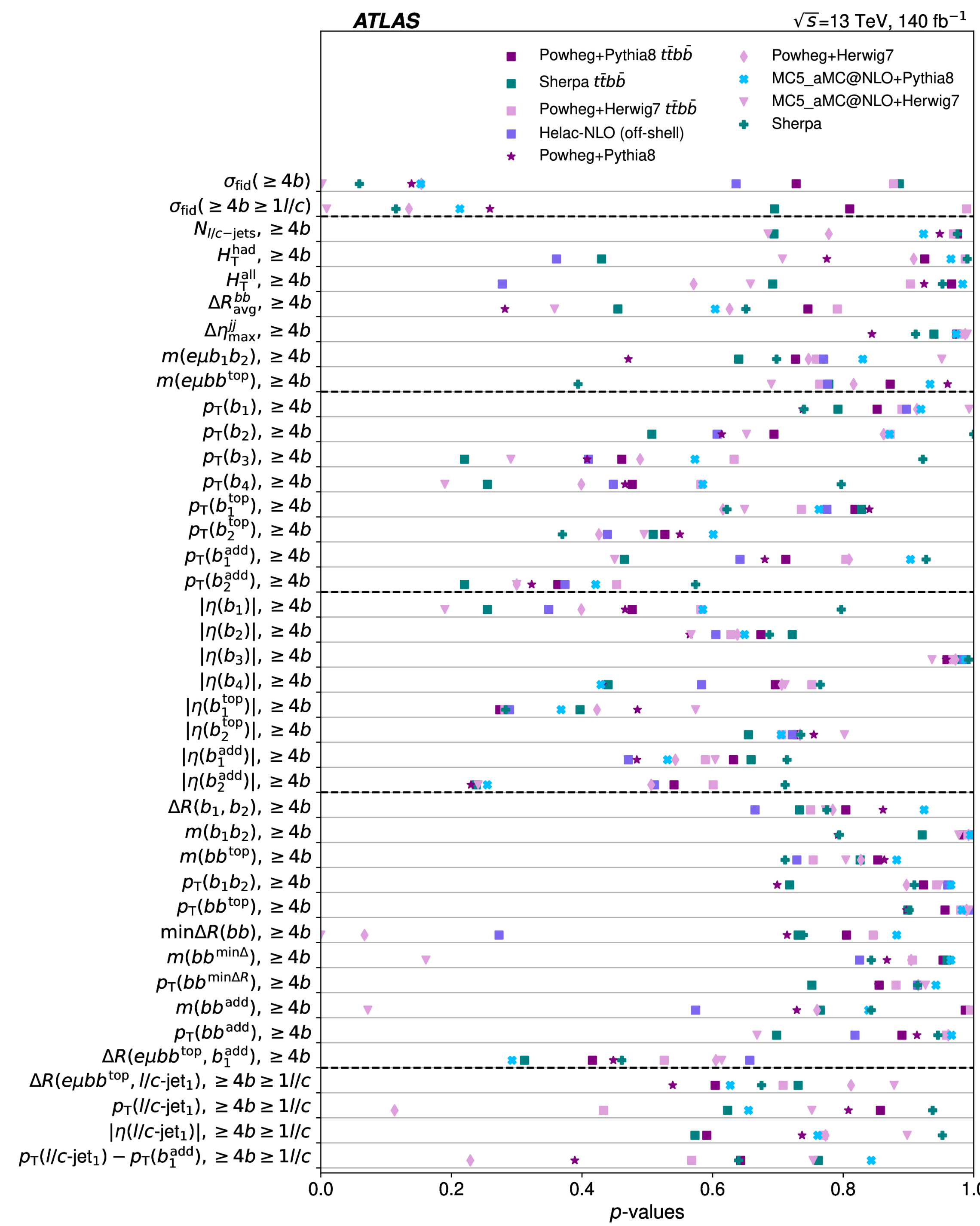

arXiv:2407.13473

ATLAS Unfolded b-jets Multiplicity

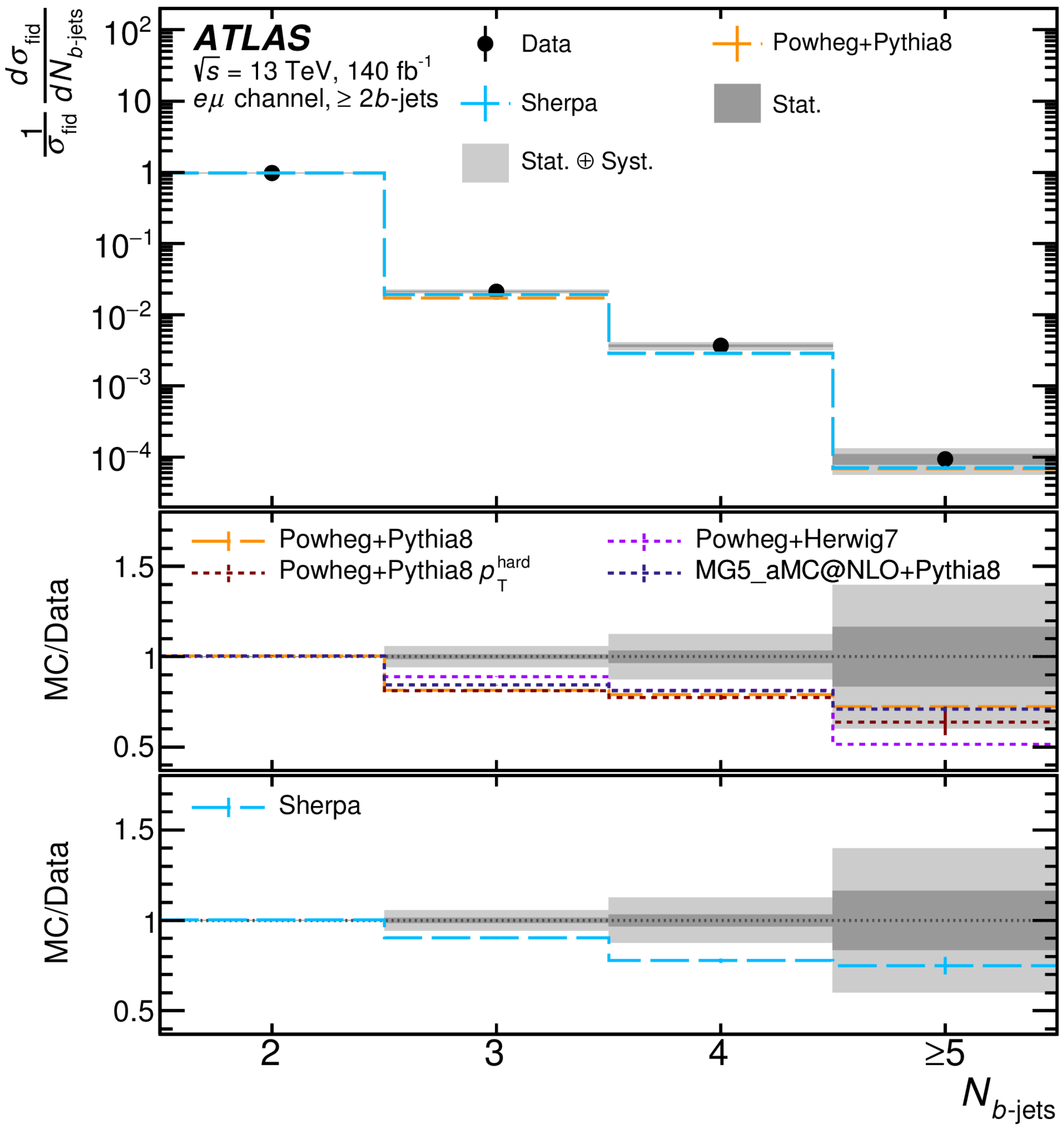

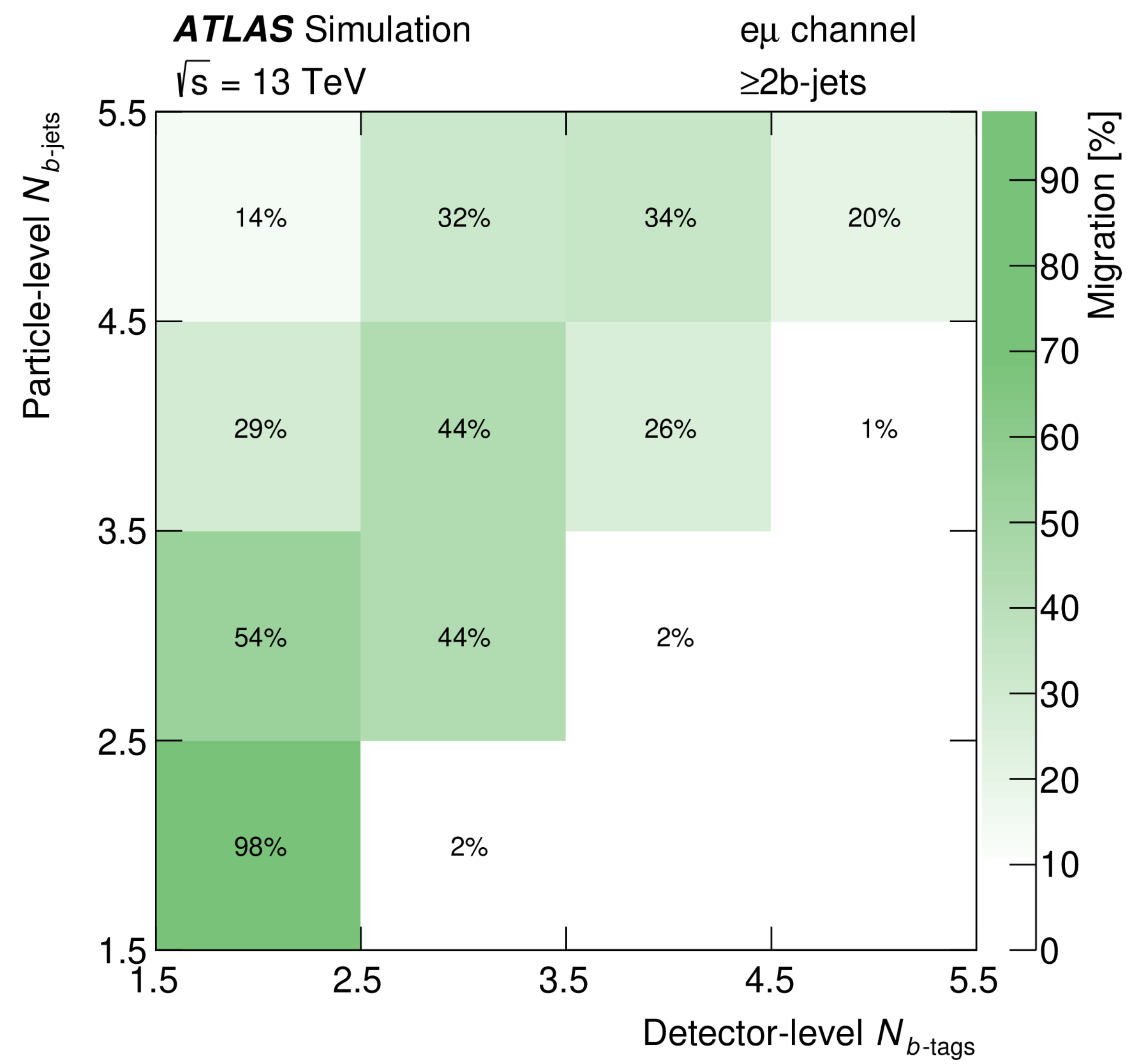

$N_{b\text{-jets}}$	$1000 \times \frac{1}{\sigma_{\text{fid}}} \frac{d\sigma_{\text{fid}}}{dN_{b\text{-jets}}}$
2	975.08 ± 0.34(stat) ± 1.49(syst)
3	21.17 ± 0.28(stat) ± 1.18(syst)
4	3.65 ± 0.12(stat) ± 0.44(syst)
≥ 5	0.09 ± 0.02(stat) ± 0.03(syst)

arXiv:2407.13473

ATLAS Diff X-Sec. with Poor Agreement in 3j3b

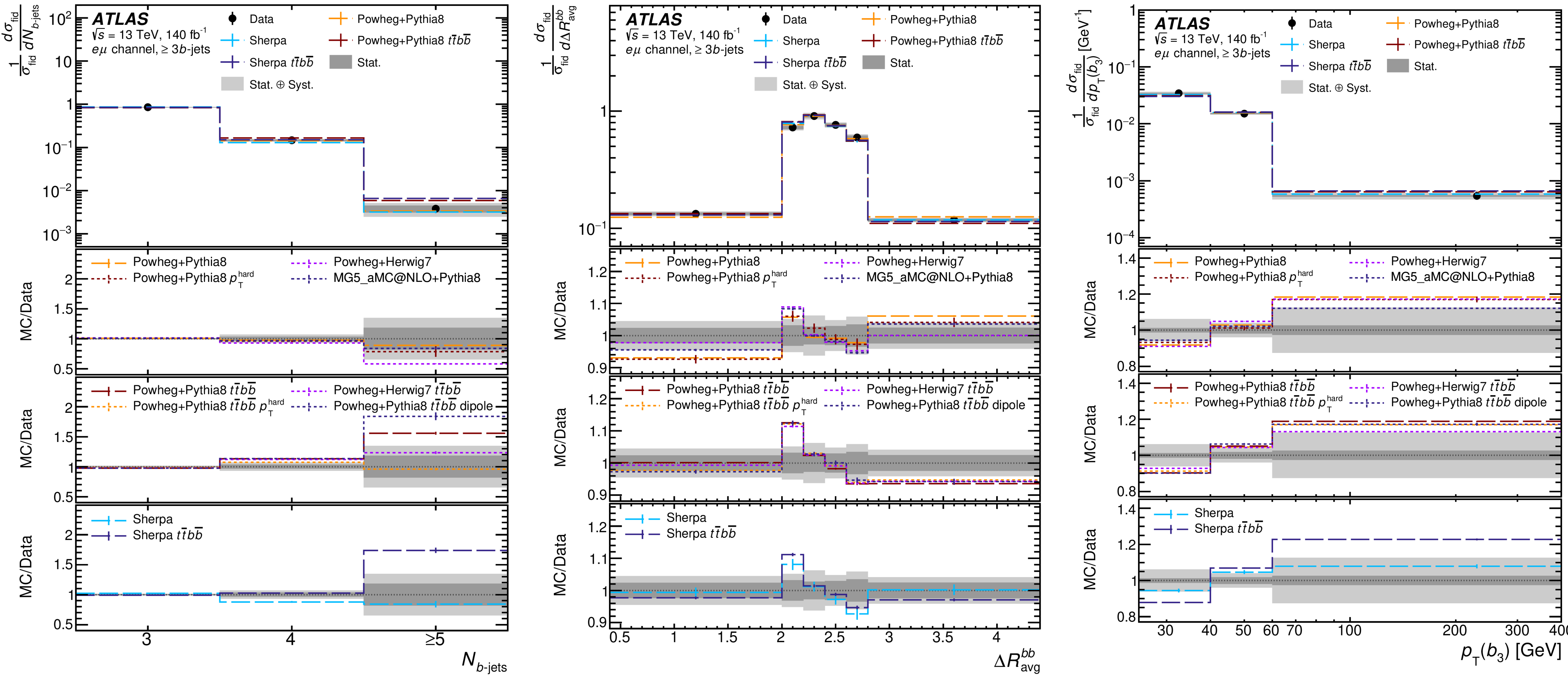

arXiv:2407.13473

ATLAS Diff X-Sec. with Poor Agreement in 3j3b

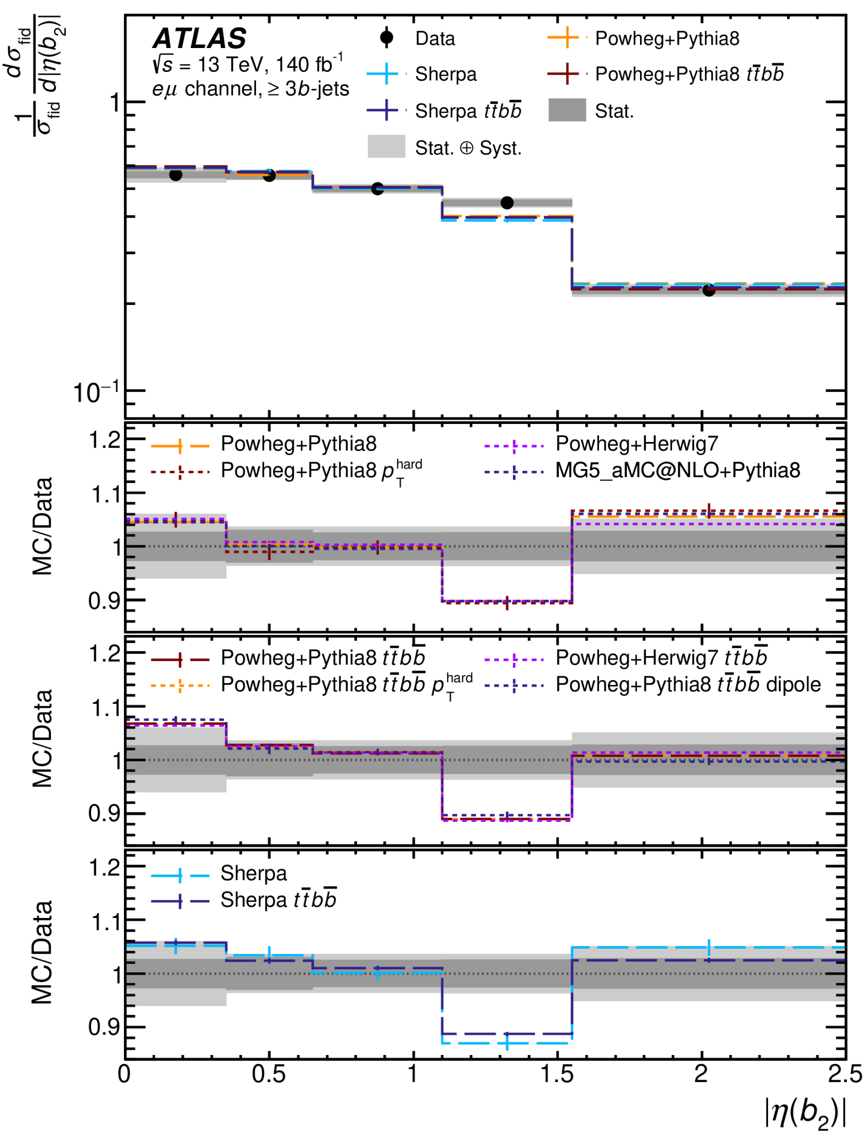

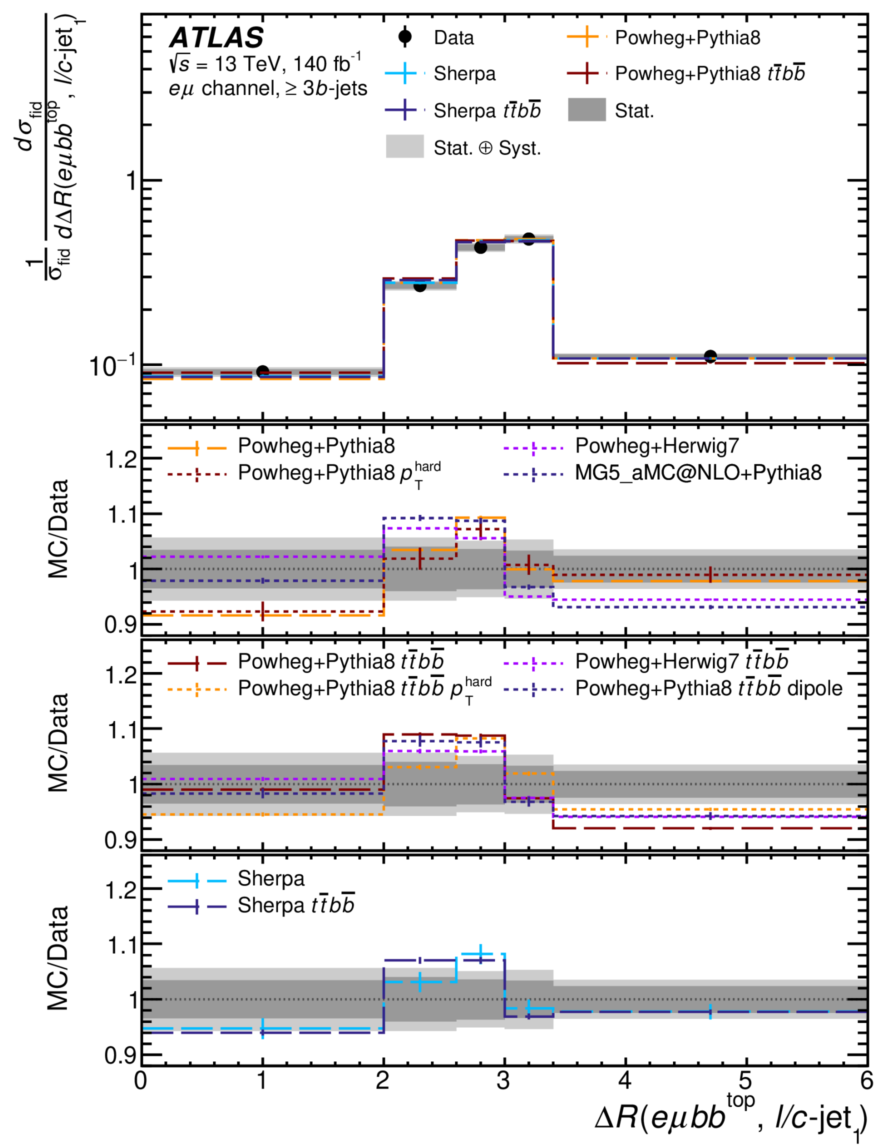

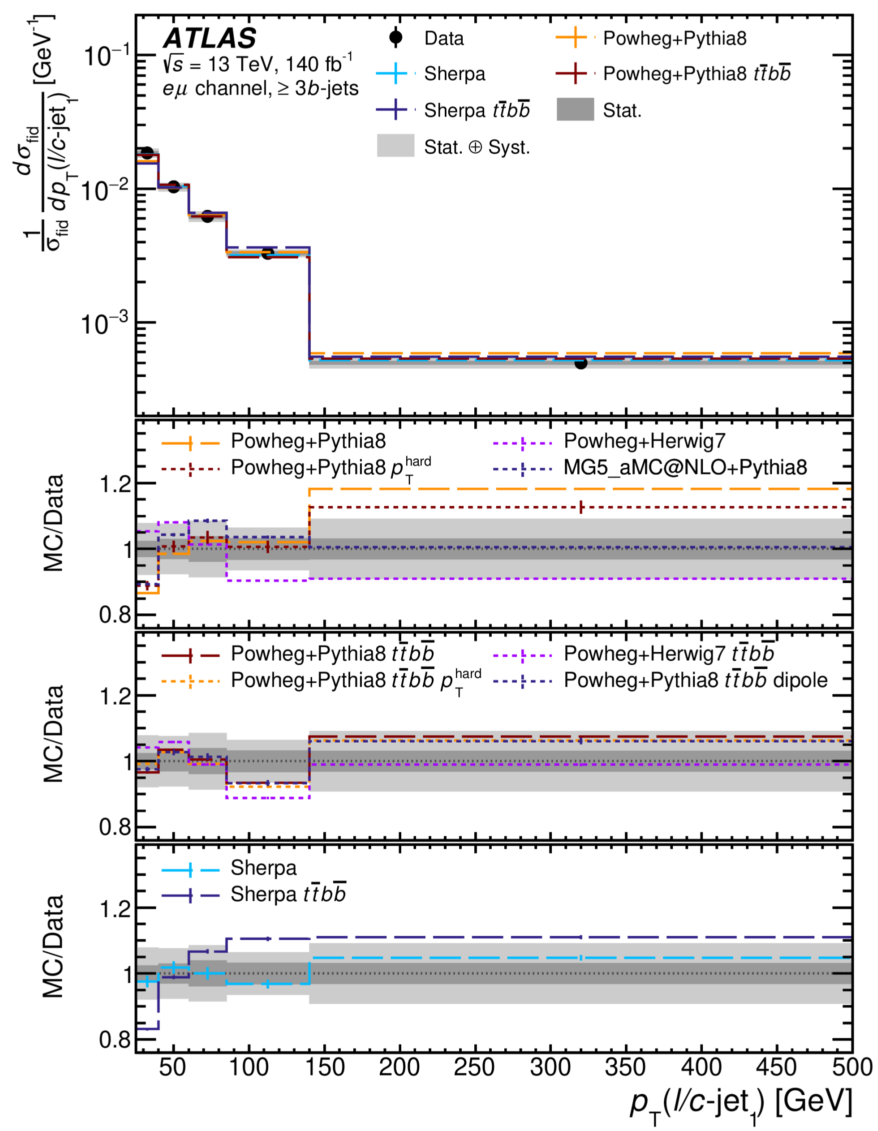

arXiv:2407.13473

ATLAS Diff X-Sec. with Poor Agreement in 3j3b

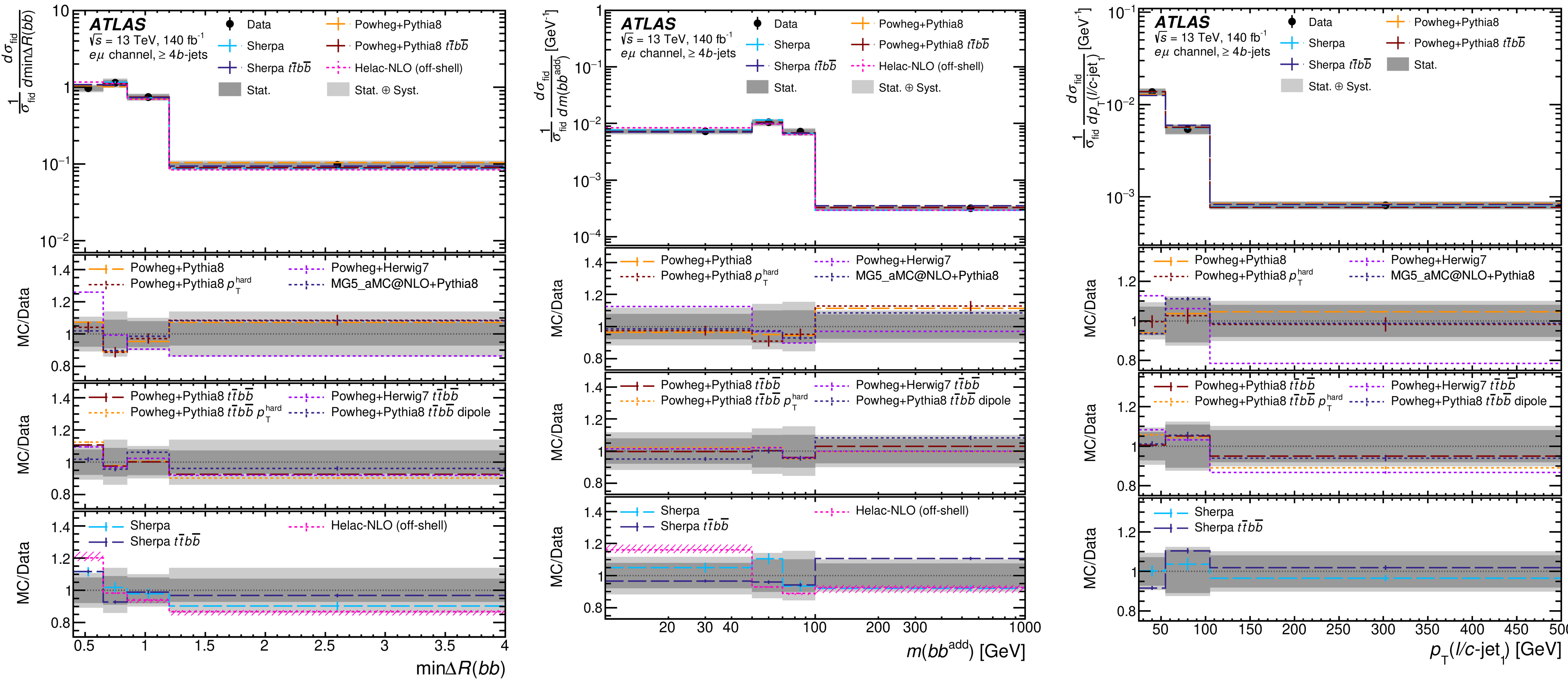

ATLAS TOPQ-2019-03
arXiv:2407.13473

CMS Signal Monte Carlo Samples

Generator settings for different modeling approaches of $\mathrm{t\bar{t}b\bar{b}}$ production. The top quark mass value set to $m_\mathrm{t} = 172.5\ \mathrm{GeV}$ for all generator setups, and for the generator setups using massive *b* quarks, the *b* quarks mass value is set to $m_\mathrm{b} = 4.75\ \mathrm{GeV}$.

Generator setup	Process/ME order	Generator/Shower	Tune	PDF set	h_damp	Scales
POWHEG+P8 $\mathrm{t\bar{t}}$ 5FS	$\mathrm{t\bar{t}}$/ NLO	POWHEG v2/ PYTHIA 8.240	CP5	5FS NNPDF3.1 NNLO	$1.379 m_\mathrm{t}$	$\mu_\mathrm{F} = \mu_\mathrm{R} = m_\mathrm{T,t}$
POWHEG+H7 $\mathrm{t\bar{t}}$ 5FS	$\mathrm{t\bar{t}}$/ NLO	POWHEG v2/ HERWIG 7.13	CH3	5FS NNPDF3.1 NNLO	$1.379 m_\mathrm{t}$	$\mu_\mathrm{F} = \mu_\mathrm{R} = m_\mathrm{T,t}$
POWHEG+OL+P8 $\mathrm{t\bar{t}b\bar{b}}$ 4FS	$\mathrm{t\bar{t}b\bar{b}}$/ NLO	POWHEG-BOX-RES/ PYTHIA 8.240	CP5	4FS NNPDF3.1 NNLO as 0118	$1.379 m_\mathrm{t}$	$\mu_\mathrm{R} = \frac{1}{2} \prod_{i=\mathrm{t,\bar{t},b,\bar{b}}} m_{\mathrm{T},i}^{1/4}$, $\mu_\mathrm{F} = H_\mathrm{T}/4$
SHERPA+OL $\mathrm{t\bar{t}b\bar{b}}$ 4FS	$\mathrm{t\bar{t}b\bar{b}}$/ NLO	SHERPA 2.2.4	SHERPA	4FS NNPDF3.0 NNLO as 0118	—	$\mu_\mathrm{R} = \prod_{i=\mathrm{t,\bar{t},b,\bar{b}}} m_{\mathrm{T},i}^{1/4}$, $\mu_\mathrm{F} = H_\mathrm{T}/2$
MG5_aMC+P8 $\mathrm{t\bar{t}b\bar{b}}$ 4FS	$\mathrm{t\bar{t}b\bar{b}}$/ NLO	MADGRAPH5_aMC@NLO v2.4.2/ PYTHIA 8.230	CP5	4FS NNPDF3.1 NNLO as 0118	—	$\mu_\mathrm{F} = \mu_\mathrm{R} = \sum m_\mathrm{T}$
MG5_aMC+P8 $\mathrm{t\bar{t}}$+jets FxFx 5FS	$\mathrm{t\bar{t}}$+jets FxFx/ NLO [$\leq$2 jets]	MADGRAPH5_aMC@NLO v2.6.1/ PYTHIA 8.240	CP5	5FS NNPDF3.1 NNLO	—	$\mu_\mathrm{F} = \mu_\mathrm{R} = \sum m_\mathrm{T}$, qCut $= 40$ GeV, qCutME $= 20$ GeV

JHEP 05 (2024) 042

CMS Measurement Objects Definitions

JHEP 05 (2024) 042

- **Primary electrons:**
  - 2016: $p_{\mathrm{T}} > 29$ GeV in $|\eta| < 2.5$,
  - 2017/18: $p_{\mathrm{T}} > 34$ GeV in $2.1 \leq |\eta| < 2.5$ and $p_{\mathrm{T}} > 30$ GeV in $|\eta| < 2.1$,
  - PL: $p_{\mathrm{T}} > 29$ GeV in $|\eta| < 2.5$ with momenta of FSR photons in $\Delta R < 0.1$ proximity.
- **Primary muons:**
  - 2016: $p_{\mathrm{T}} > 26$ GeV in $|\eta| < 2.4$,
  - 2017/18: $p_{\mathrm{T}} > 29$ GeV in $|\eta| < 2.4$,
  - PL: $p_{\mathrm{T}} > 24$ GeV in $|\eta| < 2.4$ with momenta of FSR photons in $\Delta R < 0.1$ proximity.
- **Veto leptons:**
  - used to reject events with more than one lepton,
  - $e(\mu)$: $p_{\mathrm{T}} > 15$ GeV in $|\eta| < 2.5$ (2.4) ,
  - PL $e(\mu)$: $p_{\mathrm{T}} > 15$ GeV in $|\eta| < 2.5$ (2.4) with momenta of FSR photons in $\Delta R < 0.1$ proximity,
- **Jets** (PL): $p_{\mathrm{T}} > 30(25)$ GeV in $|\eta| < 2.4$, $\Delta R \geq 0.4$ away from selected (prompt) lepton.
- ***b*-jets**: "*medium*" at $75 - 80\,\%$ identification efficiency ($> 80\,\%$ correct identification probability) and "*tight*" — at $60\,\%$ ($> 96\,\%$ correct identification probability). On the particle level, *b*-hadron matching is performed to identify the flavor.

CMS $t\bar{t}b\bar{b}$: Observables

	Observable	5j3b	6j4b	6j3b3l	7j4b3l
σ_{fid}	Inclusive cross section	✓	✓	✓	✓
Global observables					
N_{jets}	Jet multiplicity	✓	✓		
N_{b}	b jet multiplicity	✓			
H_{T}^{j}	Scalar p_{T} sum of all jets	✓	✓		
H_{T}^{b}	Scalar p_{T} sum of all b jets	✓	✓		
$H_{\text{T}}^{\text{light}}$	Scalar p_{T} sum of all light jets			✓	✓
Observables related to b jets					
$p_{\text{T}}(\text{b}_3)$	p_{T} of third hardest b jet	✓	✓		
$\|\eta(\text{b}_3)\|$	$\|\eta\|$ of third hardest b jet	✓	✓		
$p_{\text{T}}(\text{b}_4)$	p_{T} of fourth hardest b jet		✓		
$\|\eta(\text{b}_4)\|$	$\|\eta\|$ of fourth hardest b jet		✓		
Observables considering all pairs of b jets (bb)					
$\Delta R_{\text{bb}}^{\text{avg}}$	Average ΔR of all bb pairs		✓		
$m_{\text{bb}}^{\text{max}}$	Highest invariant mass among all bb pairs		✓		
Observables related to the pair of b jets closest in ΔR (bb^{extra})					
$p_{\text{T}}(\text{b}_1^{\text{extra}})$	p_{T} of leading extra b jet		✓		
$\|\eta(\text{b}_1^{\text{extra}})\|$	$\|\eta\|$ of leading extra b jet		✓		
$p_{\text{T}}(\text{b}_2^{\text{extra}})$	p_{T} of subleading extra b jet		✓		
$\|\eta(\text{b}_2^{\text{extra}})\|$	$\|\eta\|$ of subleading extra b jet		✓		
$\Delta R(\text{bb}^{\text{extra}})$	ΔR of bb^{extra} pair		✓		
$\|\eta(\text{bb}^{\text{extra}})\|$	$\|\eta\|$ of bb^{extra} pair		✓		
$m(\text{bb}^{\text{extra}})$	invariant mass of bb^{extra} pair		✓		
$p_{\text{T}}(\text{bb}^{\text{extra}})$	p_{T} of bb^{extra} pair		✓		
Observables related to the pair of b jets not from $t\bar{t}$ decay ($\text{bb}^{\text{add.}}$)					
$p_{\text{T}}(\text{b}_1^{\text{add.}})$	p_{T} of leading additional b jet		✓*		
$\|\eta(\text{b}_1^{\text{add.}})\|$	$\|\eta\|$ of leading additional b jet		✓*		
$p_{\text{T}}(\text{b}_2^{\text{add.}})$	p_{T} of subleading additional b jet		✓*		
$\|\eta(\text{b}_2^{\text{add.}})\|$	$\|\eta\|$ of subleading additional b jet		✓*		
$\Delta R(\text{bb}^{\text{add.}})$	ΔR of $\text{bb}^{\text{add.}}$ pair		✓*		
$\|\eta(\text{bb}^{\text{add.}})\|$	$\|\eta\|$ of $\text{bb}^{\text{add.}}$ pair		✓*		
$m(\text{bb}^{\text{add.}})$	invariant mass of $\text{bb}^{\text{add.}}$ pair		✓*		
$p_{\text{T}}(\text{bb}^{\text{add.}})$	p_{T} of $\text{bb}^{\text{add.}}$ pair		✓*		
Observables related to extra light jets					
$p_{\text{T}}(\text{lj}_1^{\text{extra}})$	p_{T} of leading extra light jet			✓	✓
$\|\Delta\phi(\text{lj}_1^{\text{extra}}, \text{b}_{\text{soft}})\|$	$\Delta\phi$ of leading extra light jet and softest b jet			✓	✓

JHEP 05 (2024) 042

CMS Unfolding Methodology I

Unfolding is performed through a maximum likelihood fit. JHEP 05 (2024) 042

The values of the particle-level cross sections which maximize the agreement between the predicted detector-level distributions and the observed data are determined from the fit. In these models, freely floating parameters of interest determine the total cross section of the signal process in the corresponding phase space, as well as the normalized differential cross section of the signal process in discrete bins of the considered observable.

The electron and muon channels as well as the four data-taking eras and the ancillary variable regions are combined at the likelihood level:

$$L(\vec{\mu},\vec{\alpha}) = \left[\prod_{e,i} \mathrm{Poi}\left(D_{e,i} \middle| S_{e,i}(\vec{\mu},\vec{\alpha}) + \sum_{p\in\mathrm{bkg.}} N^{p}_{e,i}(\vec{\alpha})\right)\right] \mathcal{N}(\vec{\alpha})$$

where $\vec{\mu}$ are freely-floating parameters of interest, $\vec{\alpha}$ are profiled nuisance parameters used to model systematic uncertainties, $D_{e,i}$ are the observed yield in data-taking era e and detector-level bin i, $N^{p}_{e,i}$ are the predicted yields of background process p in era e and bin i, $S_{e,i}$ are the predicted signal yields in in era e and bin i, $\mathrm{Poi}(d\,|\,\nu)$ is the Poisson probability mass function for counts d with mean ν, and $\mathcal{N}(\vec{\alpha})$ is the Gaussian constant term (with mean of zero and width of one of the nuisance) parameters.

CMS Unfolding Methodology II

The expected event yields in era e is: $M^e_{ij} = \mathscr{L}_e \sigma^0_j K^e_{ij}$, JHEP 05 (2024) 042

where $\mathscr{L}_e$ is the integrated luminosity in era e, σ^0_j is the profit cross section in bin j estimated using the nominal $\mathrm{t\bar{t}b\bar{b}}$ sample, and K^e_{ij} are response matrices.

The total expected signal yields S are computed as functions of the parameter of interest as:

$$S_{e,i}(\vec{\mu}, \vec{\alpha}) = \mu_{\mathrm{fid}} \sum_{j=1}^{n} \mu_j M^e_{ij}(\vec{\alpha})$$

where $\mu_{\mathrm{fid}} = \sigma_{\mathrm{fid}}/\sigma^0_{\mathrm{fid}}$ is the signal-strength modifier for the inclusive cross section, and μ_j are the parameters varying the fraction of signal events in each generator-level bin j. TO preserve unity, the yields in the last generator-level bin n are not scaled independently, but as a function of the other bins:

$$\mu_n(\mu_1 \ldots \mu_{n-1}) = \frac{1}{F_n}\left(1 - \sum_{i=1}^{n-1} \mu_i F_i\right)$$

where $F_j = \sigma^0_j/\sigma^0_{\mathrm{fid}} = \sigma^0_j/\Sigma^n_{i=i}\sigma^0_i$ is the *a priory* fractional cross section in bin j. The measured inclusive cross section is directly obtained as $\hat{\sigma}_{\mathrm{fid}} = \hat{\mu}_{\mathrm{fid}}\sigma^0_{\mathrm{fid}}$. The measured normalized differential cross section in bin j is extracted as $1/\hat{\sigma}_{\mathrm{fid}}\mathrm{d}\hat{\sigma}_j/\mathrm{dX} = \hat{\mu}_j F_j/w_j$, where w_j us the width f generator-level bin j.

CMS Fiducial Cross-Section Measurements: Results

Measured and predicted inclusive cross sections

Fiducial phase space	5j3b	6j3b3l	6j4b	7j4b3l
Measured cross section	2367 ± 142 (syst) ± 14 (stat)	1037 ± 90 (syst) ± 12 (stat)	291 ± 36 (syst) ± 6 (stat)	147 ± 24 (syst) ± 5 (stat)
POWHEG+OL+P8 $t\bar{t}b\bar{b}$ 4FS	2361	1183	361	197
μ_R variation	+1161/−737	+826/−433	+183/−113	+121/−67
μ_F variation	+126 /−100	+97 /−78	+23 /−18	+16 /−13
POWHEG+P8 $t\bar{t}$ 5FS	1791	899	240	129
POWHEG+H7 $t\bar{t}$ 5FS	1665	762	197	95
SHERPA+OL $t\bar{t}b\bar{b}$ 4FS	1391	677	216	116
MG5_aMC+P8 $t\bar{t}b\bar{b}$ 4FS	1024	524	187	101
MG5_aMC+P8 $t\bar{t}$+jets FxFx 5FS	1560	712	203	101

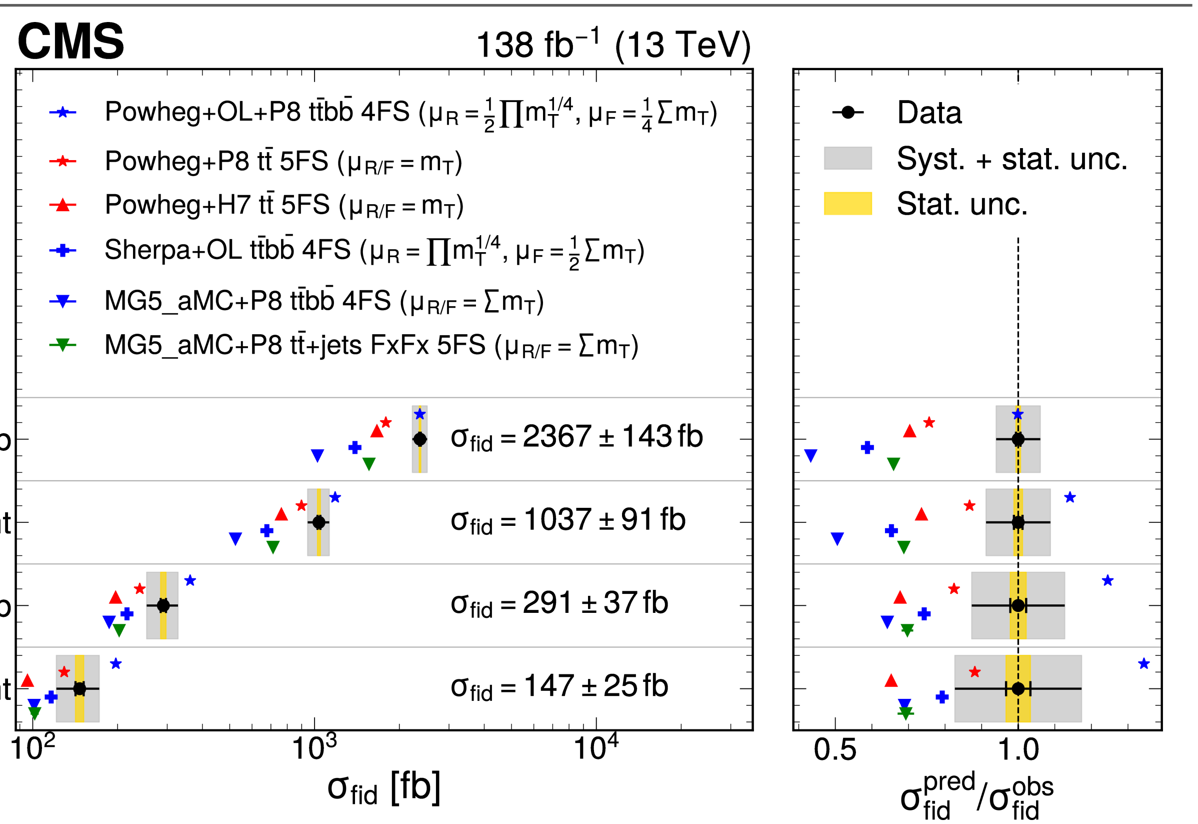

JHEP 05 (2024) 042

Contributions of the considered sources of uncertainty to the total uncertainty in the inclusive cross section measurement

Uncertainty source	Relative uncertainty (%) 5j3b	6j3b3l	6j4b	7j4b3l
Integrated luminosity	1.6	1.6	2.0	1.8
Pileup reweighting	0.2	0.8	0.4	0.5
Lepton and trigger	1.1	0.9	1.9	1.8
JES, JER	2.1	1.6	3.5	5.7
b tagging	4.5	3.9	7.0	9.1
μ_R and μ_F scales	2.8	6.8	8.2	12
Top quark p_T modelling	0.3	1.0	0.6	1.3
PDF	0.2	0.7	1.0	1.9
PS scales	2.8	2.7	2.4	1.5
ME-PS matching (h_{damp})	0.4	0.9	1.3	2.8
Underlying event	0.4	<0.1	0.4	0.4
Colour reconnection	1.1	1.5	1.9	4.5
b quark fragmentation	0.3	0.4	0.4	0.4
Inclusive $t\bar{t}C$ cross section	0.5	0.3	1.9	2.6
MC statistical	0.8	1.6	2.4	2.8
Total systematic uncertainty	6.0	8.7	13	17
Statistical uncertainty	0.6	1.2	2.2	3.3
Total uncertainty	6.0	8.8	13	17

The leading systematic uncertainties originate from the calibration of the *b*-tagging and of the JES, the choice of μ_R scale in the signal $t\bar{t}b\bar{b}$ and background $t\bar{t}$ processes

CMS Post-fit Nuisance Parameters Values

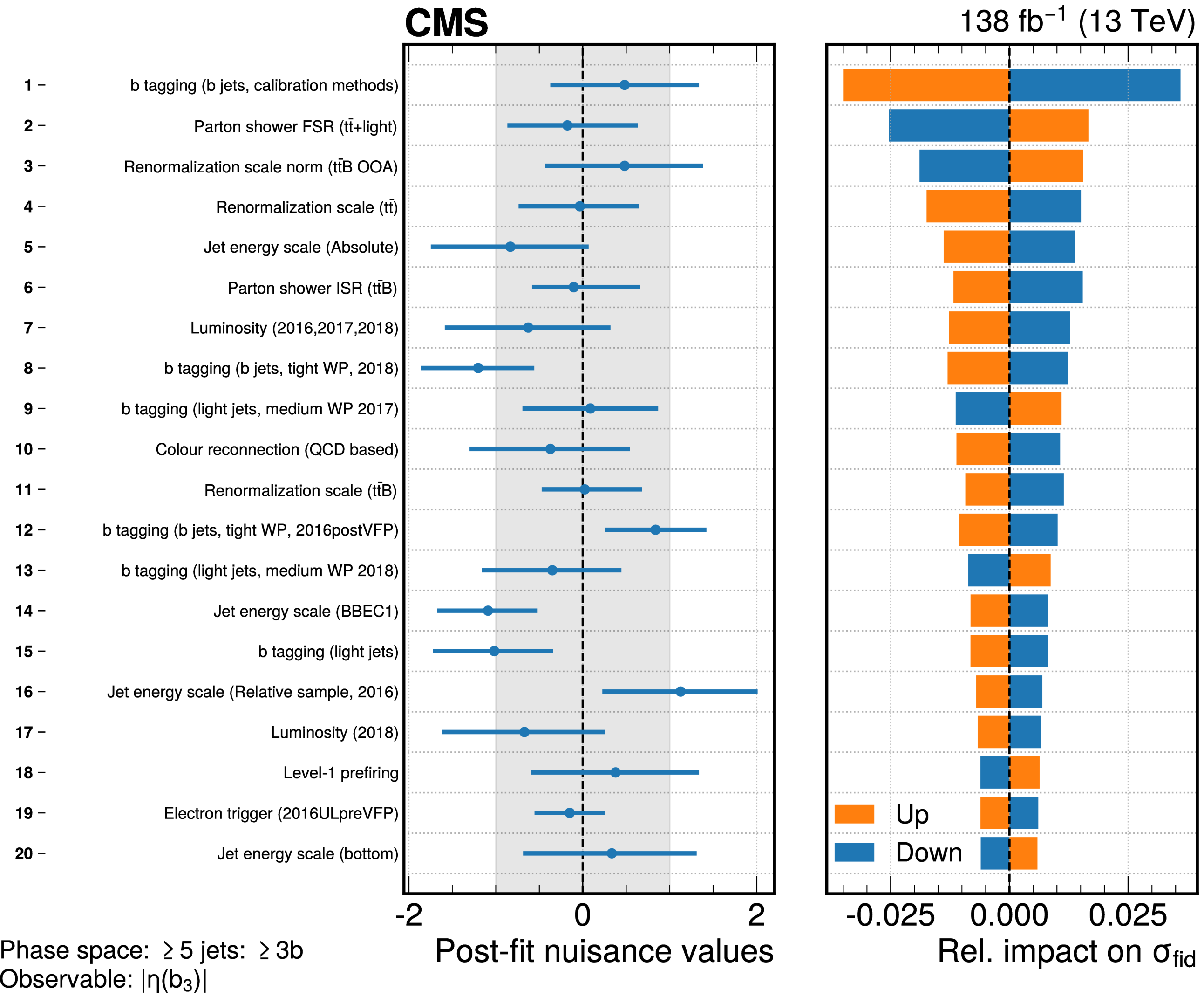

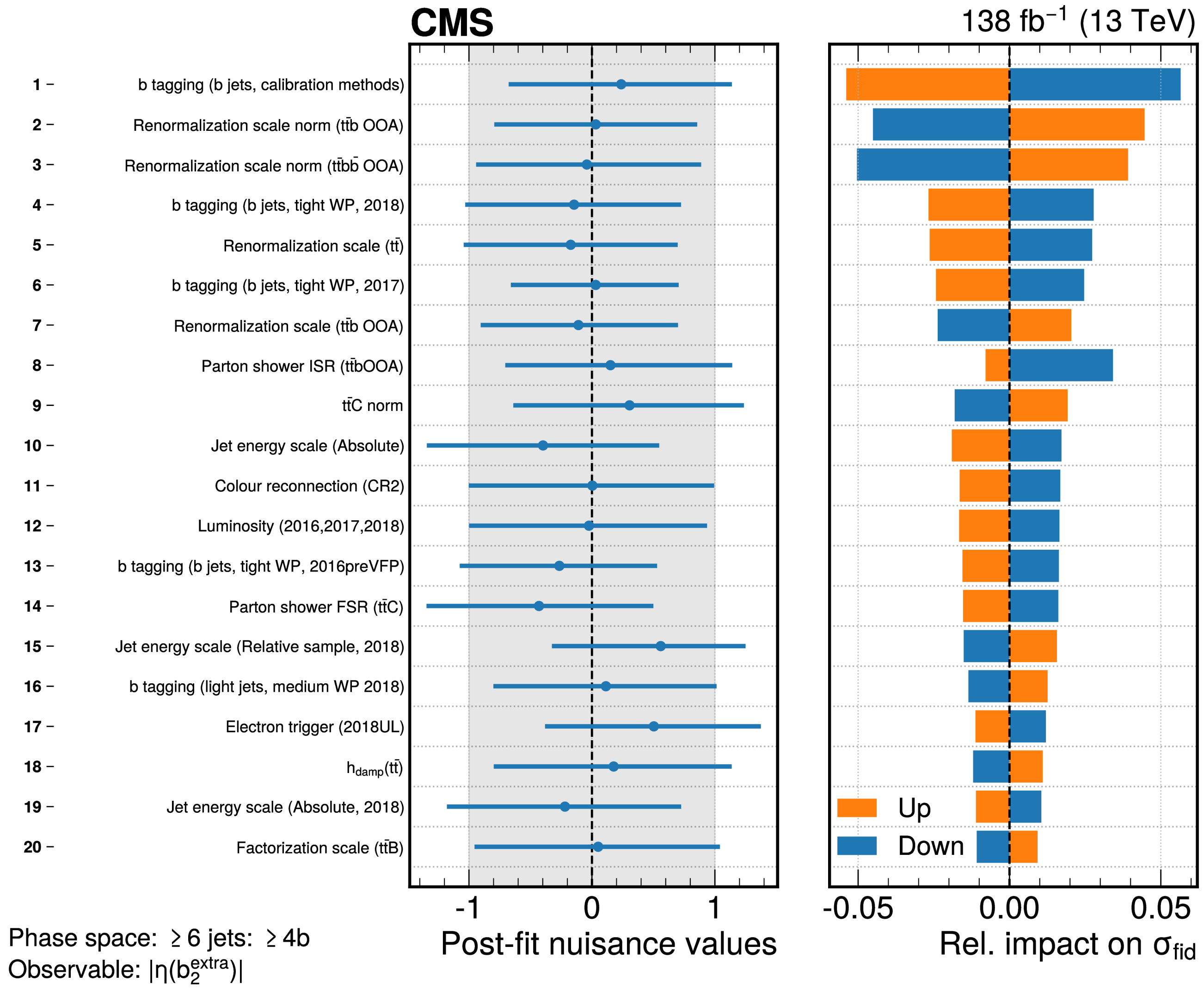

CMS Post-fit Nuisance Parameters Values

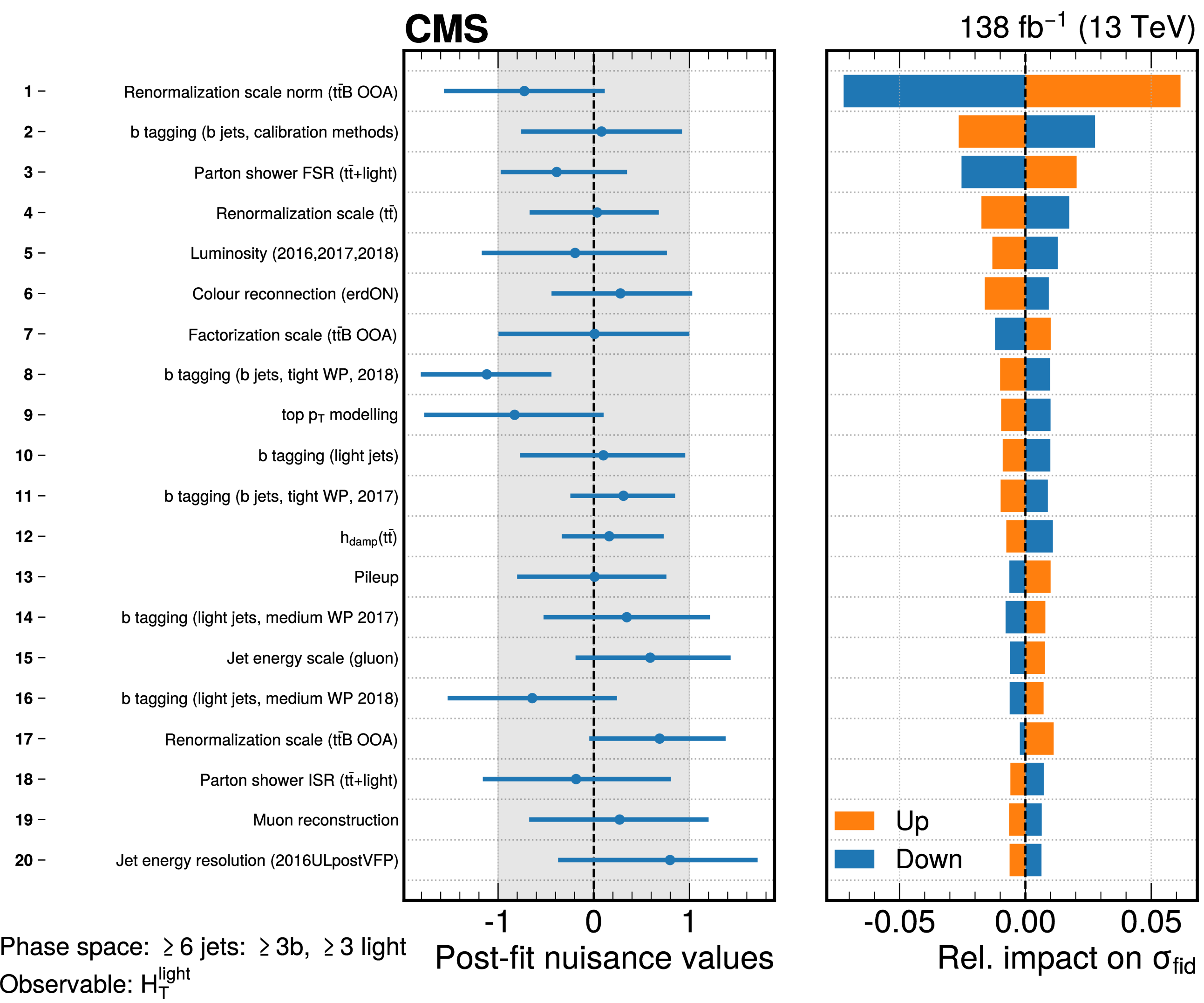

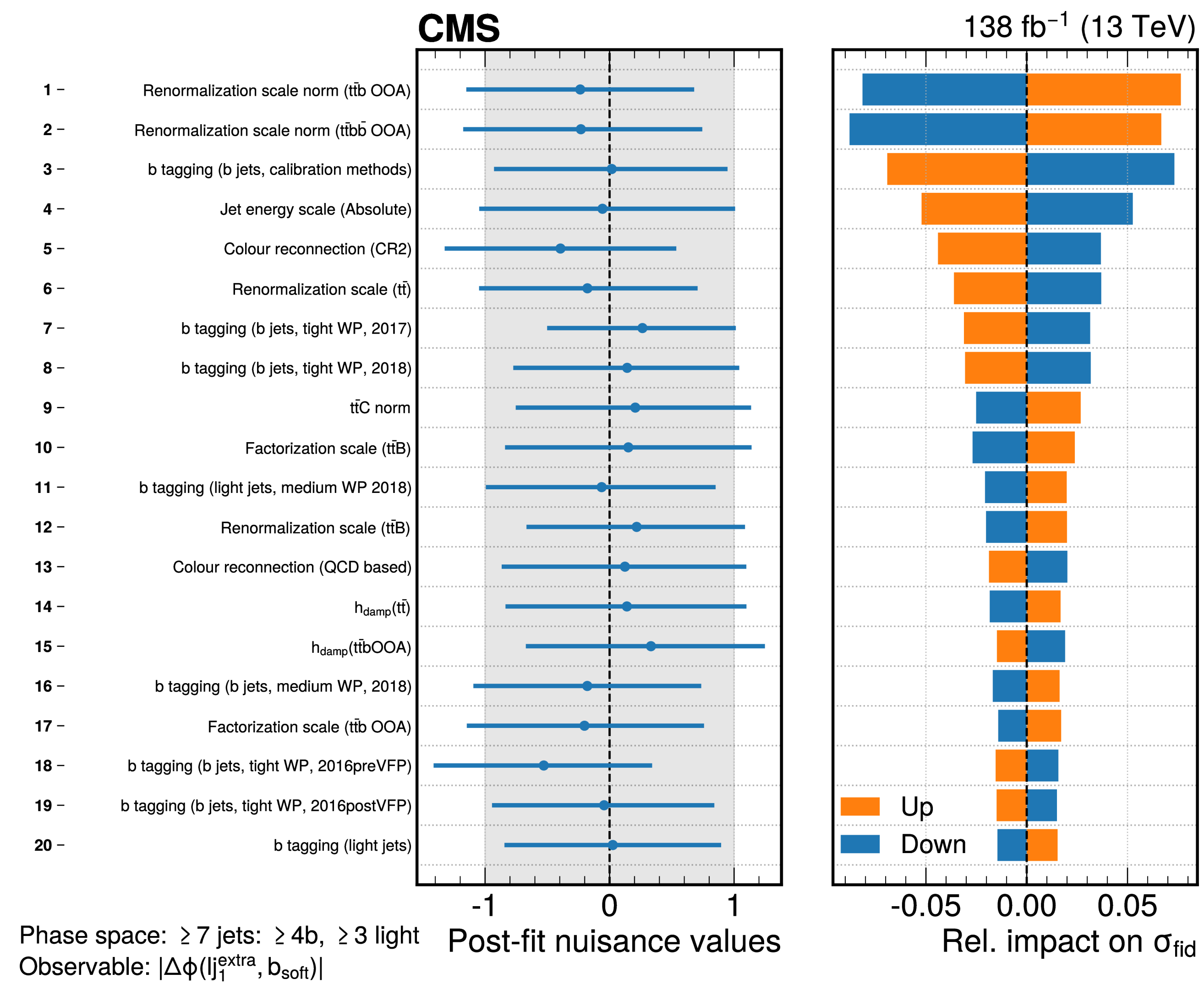

CMS Unfolded $\Delta R(bb^{extra})$ in 6j4b Region

An example of differential measurement of $\Delta R(bb^{extra})$ in 6j4b region is presented.

The response matrix (top) is averaged across eras and lepton channels, and normalized to generated-level bins (i.e. columns).

Table: z scores are estimated, most of the generators perform well with Powheg+OL+P8 $t\bar{t}b\bar{b}$ being the best for $\Delta R(bb^{extra})$.

More results (histograms and tables) are in the paper.

6j4b phase space	Observed z score: $\Delta R(bb^{extra})$	$m(bb^{extra})$	$p_T(bb^{extra})$	$p_T(b_1^{extra})$	$p_T(b_2^{extra})$	$\lvert\eta(b_1^{extra})\rvert$	$\lvert\eta(b_2^{extra})\rvert$	$\lvert\eta(bb^{extra})\rvert$
MG5_aMC+P8 $t\bar{t}$+jets FxFx 5FS	1.31	0.56	0.42	0.27	0.63	0.76	0.17	0.51
MG5_aMC+P8 $t\bar{t}b\bar{b}$ 4FS	0.23	−0.02	0.50	0.52	−0.56	0.38	−0.95	0.62
POWHEG+H7 $t\bar{t}$ 5FS	3.17	1.60	1.00	1.41	0.26	0.47	−0.39	0.88
POWHEG+OL+P8 $t\bar{t}b\bar{b}$ 4FS	−0.79	−0.69	0.60	1.05	−0.19	−0.31	−1.15	0.38
POWHEG+P8 $t\bar{t}$ 5FS	1.33	0.07	0.85	1.24	−0.19	0.03	−1.25	1.07
SHERPA+OL $t\bar{t}b\bar{b}$ 4FS	0.03	−0.99	0.95	1.12	−0.52	0.13	−1.02	0.40

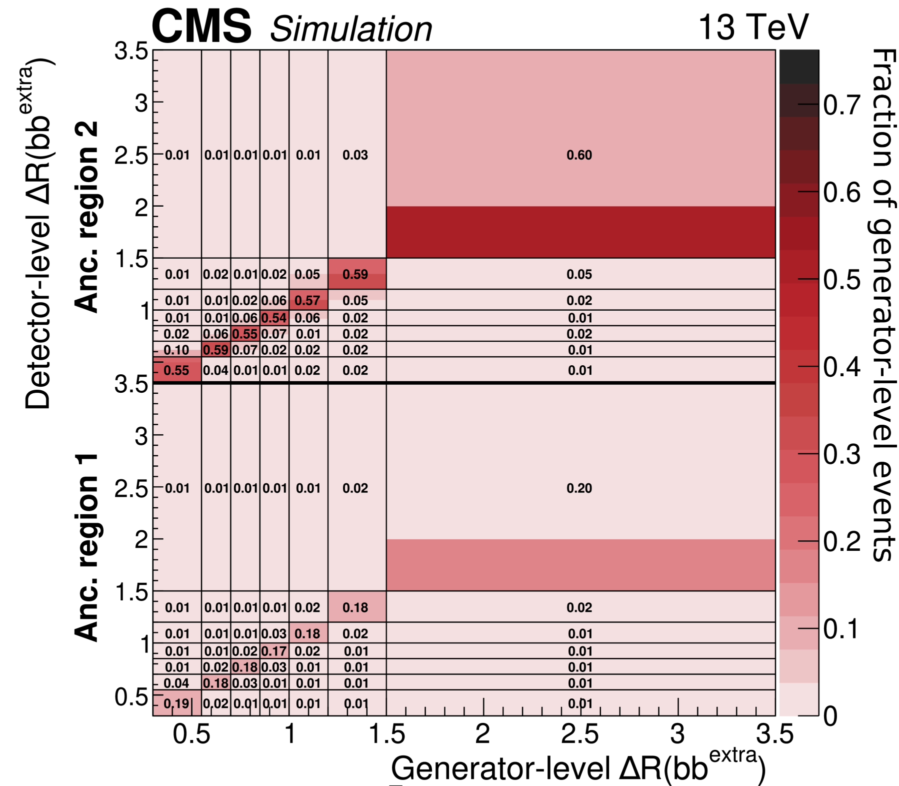

Signal model: Powheg+OL+P8 $t\bar{t}b\bar{b}$ 4FS

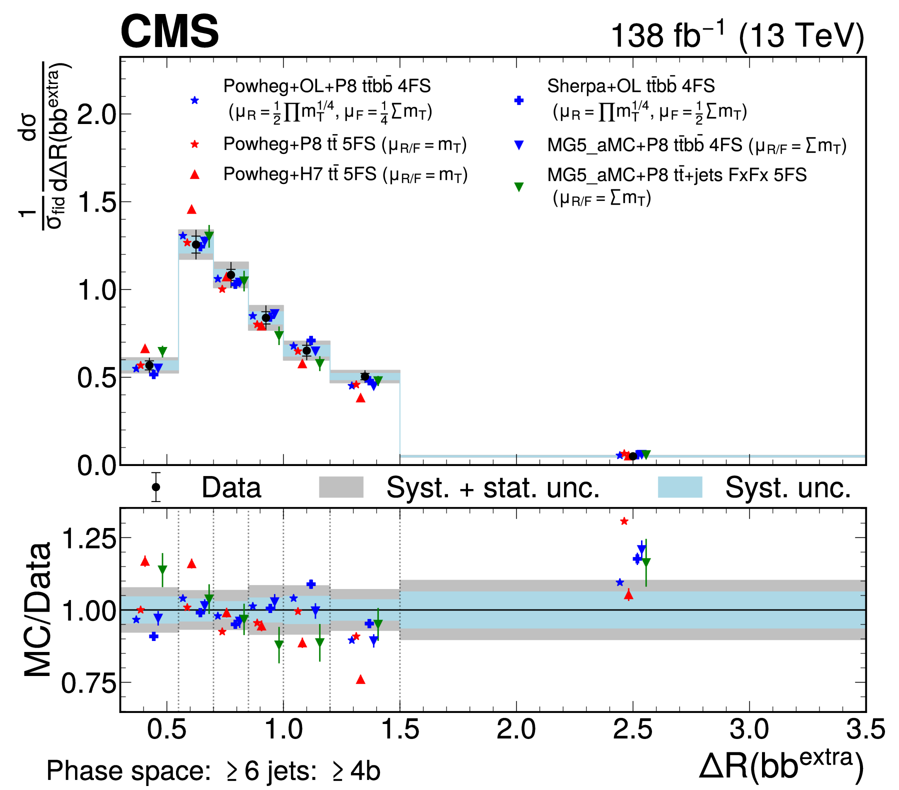

JHEP 05 (2024) 042